

RESEARCH ARTICLE

Gene-environment interaction impacts on heart development and embryo survival

Julie L. M. Moreau^{1,2}, Scott Kesteven³, Ella M. M. A. Martin¹, Kin S. Lau¹, Michelle X. Yam¹, Victoria C. O'Reilly¹, Gonzalo del Monte-Nieto^{1,2}, Antonio Baldini⁴, Michael P. Feneley^{2,3,5}, Anne M. Moon⁶, Richard P. Harvey^{1,2,7}, Duncan B. Sparrow^{1,8,*}, Gavin Chapman^{1,2,*} and Sally L. Dunwoodie^{1,2,7,†}

ABSTRACT

Congenital heart disease (CHD) is the most common type of birth defect. In recent years, research has focussed on identifying the genetic causes of CHD. However, only a minority of CHD cases can be attributed to single gene mutations. In addition, studies have identified different environmental stressors that promote CHD, but the additive effect of genetic susceptibility and environmental factors is poorly understood. In this context, we have investigated the effects of short-term gestational hypoxia on mouse embryos genetically predisposed to heart defects. Exposure of mouse embryos heterozygous for *Tbx1* or *Fgfr1/Fgfr2* to hypoxia *in utero* increased the incidence and severity of heart defects while *Nkx2-5*^{+/-} embryos died within 2 days of hypoxic exposure. We identified the molecular consequences of the interaction between *Nkx2-5* and short-term gestational hypoxia, which suggest that reduced *Nkx2-5* expression and a prolonged hypoxia-inducible factor 1 α response together precipitate embryo death. Our study provides insight into the causes of embryo loss and variable penetrance of monogenic CHD, and raises the possibility that cases of foetal death and CHD in humans could be caused by similar gene-environment interactions.

KEY WORDS: Congenital heart disease, Embryogenesis, Gene-environment, Gestation, Heart, Hypoxia

INTRODUCTION

Congenital heart disease (CHD), defined as a gross structural abnormality of the heart, is the most common type of human birth defect, occurring in ~9 per 1000 live births and at a significantly greater incidence in miscarriage and still births (Hoffman, 1995; van der Linde et al., 2011). Although genetic factors have been widely investigated, only a minority of cases can be attributed to a specific

genetic cause, with at least one hundred genes implicated (Blue et al., 2012). The complexity in understanding the causes of CHD is heightened by disease variability influenced by genetic, epigenetic and/or environmental modifiers. Even in families with a known monogenic cause, heart defects can show highly variable penetrance and expressivity between individuals (reviewed by Prendiville et al., 2014). Well-recognised nongenetic causes of CHD include: environmental teratogens, such as dioxins or pesticides; maternal exposures to alcohol, isotretinoin, thalidomide or anti-seizure medications; diabetes; and infectious agents such as rubella or influenza (Dewan and Gupta, 2012; Kopf and Walker, 2009; Liang et al., 2017; Ramakrishnan et al., 2015; Wren et al., 2003; Zhu et al., 2009). Additional teratogens, such as smoking, obesity and high altitude are associated with CHD, and have links to lowered oxygen (Chun et al., 2018; Sullivan et al., 2015; Webster et al., 2014; Yu et al., 2006; Zheng et al., 2013). In this study, we chose to experimentally investigate gestational hypoxia as a cause and a modifying factor of CHD.

Experimentally, hypoxia has been studied as a disruptor of embryogenesis for almost 200 years, causing a variety of birth defects, including heart defects (Ingalls et al., 1952; Saint Hilaire, 1820). We have previously shown that short-term gestational hypoxia inhibits fibroblast growth factor (FGF) signalling in the vertebral precursors (presomitic mesoderm), and increases the penetrance and expressivity of vertebral defects in mouse models of congenital scoliosis (Sparrow et al., 2012). We have also recently shown that gestational hypoxia disrupts heart development in mouse embryos by inhibiting FGF signalling in the cardiac progenitor cells of the second heart field (SHF) (Shi et al., 2016). In this context, we hypothesised that some genetically susceptible individuals might not develop CHD unless exposed to a 'second hit' environmental factor.

Here, we have investigated the effects of short-term gestational hypoxia in mouse embryos carrying null mutations in genes required for FGF signalling in the SHF (*Fgf8*, *Fgfr1* and *Fgfr2*) or associated with CHD in humans, including crucial transcription factors (*Tbx1*, *Tbx5* and *Nkx2-5*). *Fgf8*, *Fgfr1* and *Fgfr2* are expressed in the SHF, and are required for FGF signalling, proliferation of cardiac progenitor cells, and development of the outflow tract (OFT), atria and right ventricle in mice (Marguerie et al., 2006; Park et al., 2008; Watanabe et al., 2010). *Tbx1* and *Tbx5* encode T-box transcription factors. *Tbx1* is expressed in the pharyngeal mesoderm and is required for inflow as well as outflow tract morphogenesis (Rana et al., 2014). Decreased *TBX1* function accounts for many of the clinical features of chromosome 22q11 deletion syndromes in humans (Yagi et al., 2005). *Tbx5* is expressed in the inflow tract, atria and left ventricle but not in the outflow tract or the right ventricle (Bruneau et al., 1999). *Tbx5*-null mice have severe left ventricular hypoplasia and die at approximately

¹Developmental and Stem Cell Biology Division, Victor Chang Cardiac Research Institute, Darlinghurst, New South Wales 2010, Australia. ²St Vincent's Clinical School, University of New South Wales, Kensington, New South Wales 2010, Australia. ³Cardiac Physiology and Transplantation Division, Victor Chang Cardiac Research Institute, Darlinghurst, New South Wales 2010, Australia. ⁴Dept. of Molecular Medicine and Medical Biotechnologies, University Federico II, Naples, and Institute of Genetics and Biophysics, CNR, Via Pietro Castellino 111, 80131 Naples, Italy. ⁵Cardiology Department, St. Vincent's Hospital, Darlinghurst, New South Wales 2010, Australia. ⁶Department of Molecular and Functional Genomics, Weis Center for Research, Geisinger Clinic, Danville, PA 17822, USA. ⁷School of Biotechnology and Biomolecular Science, University of New South Wales, Kensington, New South Wales 2033, Australia. ⁸Department of Physiology, Anatomy and Genetics, University of Oxford, Oxford OX1 3PT, UK.

*These authors contributed equally to this work

†Author for correspondence (s.dunwoodie@victorchang.edu.au)

© J.L.M.M., 0000-0003-1559-7703; E.M.M.A.M., 0000-0001-9511-9175; G.d.M.-N., 0000-0003-3830-2226; A.B., 0000-0002-5330-0256; D.B.S., 0000-0002-1141-6613; G.C., 0000-0002-3513-723X; S.L.D., 0000-0002-2069-7349

embryonic day (E) 9 with no heartbeat (Bruneau et al., 2001). Importantly, presumed null *TBX5* mutations in humans cause Holt-Oram syndrome, which is characterised by skeletal and cardiac defects, including atrial septal defects (ASDs), ventricular septal defects (VSDs) and tetralogy of Fallot (TOF) (Newbury-Ecob et al., 1996). *Nkx2-5* encodes an NK-2 homeodomain-containing transcription factor that is expressed in cardiac progenitor cells of both the first heart field and the SHF, contributing to different parts of the heart (reviewed by Buckingham et al., 2005). In mice, loss of *Nkx2-5* results in embryonic lethality around E9.5 that is associated with cardiac developmental arrest involving abnormal looping, inhibited contribution of SHF precursors to the primary heart tube and arrested chamber development, highlighting its central importance for heart development (Prall et al., 2007). Furthermore, *Nkx2-5* is essential for the formation, maturation and maintenance of the conduction system, as well as for myocardial contractility (Biben et al., 2000; Briggs et al., 2008). More than 40 mutations of the *NKX2-5* gene have been identified in CHD patients with various clinical phenotypes, including ASDs, VSDs, TOF, patent ductus arteriosus (PDA), hypoplastic left heart and dilated cardiomyopathy (Benson, 2010; Reamon-Buettner and Borlak, 2010). Such variability is evident even within families (Benson, 2010; Benson et al., 1999; Reamon-Buettner and Borlak, 2010).

We show that short-term gestational hypoxia can increase the severity and incidence of heart defects in genetically susceptible embryos. We also show that interaction between hypoxia and *Nkx2-5* haploinsufficiency causes heart failure and embryo death, possibly due to reduced *Nkx2-5* expression and a prolonged hypoxia inducible factor 1 alpha (HIF1 α) response. These findings provide new mechanistic insights for understanding the variable penetrance and expressivity observed in cases of monogenic CHD, and how *in utero* hypoxia might contribute to sporadic cases of CHD and miscarriage.

RESULTS

Redundancy in FGF receptors protects against environmentally induced heart defects

We have previously shown that short-term gestational hypoxia disrupts somitogenesis and heart development in mouse embryos by inhibiting FGF signalling in the presomitic mesoderm and in the SHF, respectively (Shi et al., 2016; Sparrow et al., 2012). We have also demonstrated a gene-environment interaction (GxE) between genetic predisposition to vertebral segmentation defects and short-term gestational hypoxia (Sparrow et al., 2012). Therefore, we hypothesised that embryos genetically susceptible to reduced FGF signalling capacity might be more vulnerable to developing heart defects if exposed to *in utero* hypoxia. The FGF8 ligand and its receptors FGFR1 and FGFR2 are required for proliferation of SHF cardiac progenitor cells (Macatee et al., 2003; Marguerie et al., 2006; Park et al., 2008; Watanabe et al., 2010). We have previously determined that the mouse embryonic heart is most vulnerable to short-term gestational hypoxia when maternal exposure commences at embryonic day (E) 9.5 (Shi et al., 2016). However, penetrance of heart defects increases as oxygen levels decrease. Maternal exposure to 5.5% oxygen for 8 h causes defects in 50% of embryos; exposure to 8% oxygen causes heart defects in ~0-12.5% of embryos; and exposure to >9% oxygen does not cause heart defects (O'Reilly et al., 2014; Shi et al., 2016). To best detect an increase in the incidence of heart defects due to GxE, we chose to expose pregnant mice to 8% oxygen. We mated heterozygous males carrying null alleles of *Fgf8*, *Fgfr1* and/or *Fgfr2* with wild-type

females to produce litters carrying both wild-type and heterozygous embryos. This breeding strategy removed any potential influence that the genotype of the mother might have on embryonic development. We exposed pregnant females to 8% oxygen for 8 h at E9.5, returned them to normoxia (21% oxygen) and harvested embryos at E17.5. Control litters were allowed to develop in normoxia throughout gestation. Heart morphology was assessed using optical projection tomography (OPT) (Fig. S1) (Shi et al., 2016). The incidence of heart defects, ranging from 0-8%, was not statistically different between *Fgf8*^{+/+} and *Fgf8*^{+/-} embryos at normoxia or 8% oxygen (Fig. S2A, Table S1). To determine whether exposure to more severe hypoxia caused a discernible GxE, we repeated the experiment by exposing pregnant mice to 5.5% oxygen. However, such exposure increased the incidence (30-39%) and severity of heart defects, including a straddling overriding tricuspid valve (SOTV), transposition of the great arteries (TGA) and *ectopia cordis*, equally in both genotypes (Fig. S2A, Table S1). For *Fgfr1* and *Fgfr2* mutants, the incidence of heart defects (0-11%) was similar between wild-type and heterozygous embryos for both normoxia and 8% oxygen (Fig. 1A, Table S1). As it is known that *Fgfr1* and *Fgfr2* function redundantly during heart formation (Park et al., 2008), we tested for GxE in embryos heterozygous null for both genes. None of the *Fgfr1*^{+/-};*Fgfr2*^{+/-} embryos had heart defects at normoxia (Fig. 1A, Table S1) but exposure to 8% oxygen caused a significant increase in the number of embryos with heart defects to 26% and increased severity due to a hypoplastic right heart (Fig. 1A). The heart defects are the same as those that result from loss of FGF signalling via either genetic or environmental disruption (Table S1; Marguerie et al., 2006; Park et al., 2008; Shi et al., 2016). These data are consistent with previous work showing redundant roles for these receptors in the SHF and demonstrate that GxE disrupts FGF signalling in the SHF and thus impacts on heart development.

GxE with genes associated with CHD leads to an increased incidence of heart defects and embryonic lethality

We next sought to investigate how short-term gestational hypoxia might modify heart phenotypes in mouse strains carrying null alleles in genes known to cause monogenic CHD in humans. We first analysed *Tbx1* and *Tbx5*, mutations in which cause DiGeorge syndrome (Chieffo et al., 1997) and Holt-Oram syndrome in humans, respectively (Li et al., 1997). We crossed either *Tbx1*^{+/-} or *Tbx5*^{+/-} males with C57BL/6J wild-type females, exposed the pregnant mice to normoxia or 8% oxygen, and analysed heart morphology as before. Under normoxic conditions ~30% of *Tbx5*^{+/-} embryos had heart defects (11/38), as previously reported (Bruneau et al., 2001), whereas all *Tbx5*^{+/+} littermates had normal hearts (Fig. S2B). The incidence was not significantly increased in either *Tbx5*^{+/-} or *Tbx5*^{+/-} embryos following maternal exposure to 8% oxygen; the types of heart defects were also unchanged, except that muscular VSDs were observed in *Tbx5*^{+/-} embryos following exposure to 8% oxygen (Fig. S2B, Table S2). The incidence of heart defects was very low (0-5%) in *Tbx1*^{+/+} and *Tbx1*^{+/-} embryos in both normoxia and 8% oxygen, consisting of either membranous VSDs or muscular VSDs (Fig. 1B, Table S2). Previously, *Tbx1*^{+/-} embryos were reported to have highly penetrant aortic arch defects (Lindsay et al., 2001); we were unable to assess heart morphology using OPT and the aortic arch simultaneously at this late stage because the aortic arch was often damaged by the animal ethics-mandated method of euthanasia (decapitation). After maternal exposure to 5.5% oxygen, the incidence of heart defects in *Tbx1*^{+/-} embryos was significantly greater (74%) than low-oxygen treatment alone (37%) (Fig. 1B,

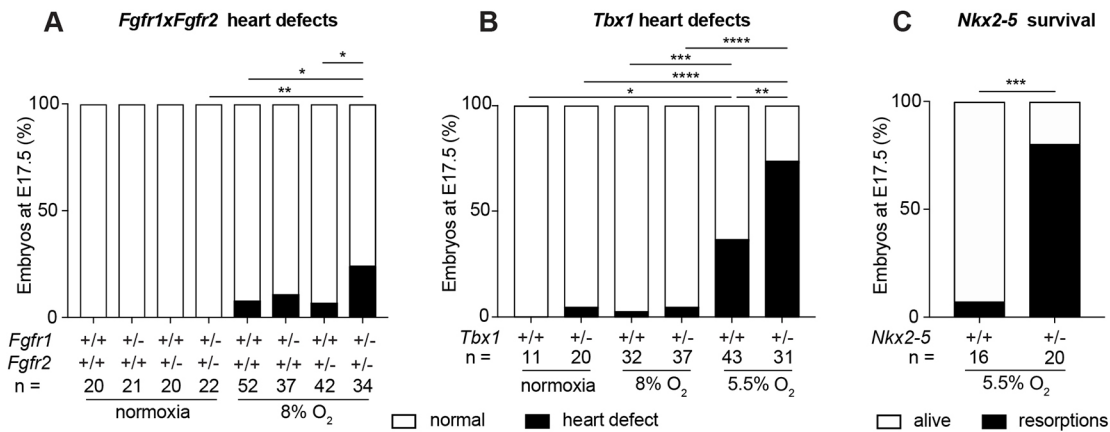


Fig. 1. Embryonic survival and incidence of heart defects in embryos with mutated cardiac development genes following maternal exposure to low oxygen. (A,B) Histograms showing the percentage of heart defects present in E17.5 embryos following maternal exposure to the indicated level of hypoxia at E9.5. (A) *Fgfr1xFgfr2* and (B) *Tbx1*. (C) Histograms showing the percentage of surviving *Nkx2-5* strain embryos following maternal exposure to the indicated level of hypoxia at E9.5. Data were tested for statistical significance using two-tailed Fisher's exact test. * $P < 0.05$, ** $P < 0.01$, *** $P < 0.001$, **** $P < 0.0001$.

Table S2), indicating a GxE. Moreover, at 5.5% oxygen, additional heart defects occurred such as TGA, overriding aorta (OA), double-outlet right ventricle (DORV) and persistent truncus arteriosus (PTA).

Finally, we analysed the *Nkx2-5* gene, which is associated with structural heart defects and defects of the cardiac conduction system, in humans (McElhinney et al., 2003; Perera et al., 2014). Only two *Nkx2-5*^{+/-} embryos exposed to 8% oxygen had a heart defect, one with a VSD and one with an ASD (Fig. S3A, Table S2). However, maternal exposure to 5.5% oxygen resulted in significant embryonic lethality in *Nkx2-5*^{+/-} embryos by E17.5 (80% *Nkx2-5*^{+/-} resorptions compared with 6% in *Nkx2-5*^{+/+}, Fig. 1C), which was not observed when embryos were exposed to 8% oxygen. Taken together, these data indicate that gestational hypoxia has variable effects on the penetrance and expressivity of heart defects in embryos of different genetic predispositions.

Hearts of *Nkx2-5*^{+/-} embryos are morphologically heterogeneous following maternal low-oxygen exposure

We pursued the basis for the severe GxE observed in *Nkx2-5* heterozygotes that leads to the high rate of embryonic lethality in these embryos. We harvested embryos at different stages after hypoxic exposure. A significant deviation from expected Mendelian ratios was evident at E11.5-E13.5 (Fig. 2A). At these stages, significantly more of the surviving embryos were *Nkx2-5*^{+/+} compared with *Nkx2-5*^{+/-} (Fig. 2A) and consistent with this, the majority of resorbed embryos that could be genotyped were *Nkx2-5*^{+/-} (Fig. S3B). By contrast, at E10.5 there were few resorptions and *Nkx2-5* embryos of both genotypes appeared to be equally represented (Fig. 2A, Fig. S3B). However, approximately half of the E10.5 *Nkx2-5*^{+/-} embryos (295/656) had a dilated heart and a pericardial effusion (Fig. 2B,E-G). Such a phenotype is often associated with cardiac insufficiency (Flores et al., 2014). All embryos had an equivalent number of somite pairs at E10.5, irrespective of treatment or genotype, indicating that hypoxia did not induce developmental delay (data not shown). By E11.5, there were no *Nkx2-5*^{+/-} embryos with dilated hearts, but many *Nkx2-5*^{+/-} embryos had died (Fig. 2B), suggesting that the dilated heart phenotype at E10.5 was evidence of lethal heart failure. Heart morphology at E10.5 was further investigated using OPT (Fig. 2H-Q). Quantification of three-dimensional models of the heart showed that *Nkx2-5*^{+/-} embryos with dilated hearts had

reduced myocardial volume and increased chamber volume compared with unexposed *Nkx2-5*^{+/+} and *Nkx2-5*^{+/-} embryos and with *Nkx2-5*^{+/-} embryos with morphologically normal hearts exposed to hypoxia (Fig. 2R-T). These results indicate that short-term gestational hypoxia induces heart dilation and pericardial effusion in about half of the *Nkx2-5*^{+/-} embryos by E10.5 and that this cardiac insufficiency leads to embryo death a day later. The remaining 50% of *Nkx2-5*^{+/-} embryos were morphologically normal at E10.5 and yet about half of them were absent by E11.5.

Embryonic *Nkx2-5* expression is affected following maternal low-oxygen exposure

We hypothesised that the cardiac phenotype and lethality observed after hypoxia in *Nkx2-5*^{+/-} embryos could be due to the effects of heterozygosity compounded by further reduction of transcript and/or protein production from the remaining functional allele due to hypoxia. To test this hypothesis, we quantified both transcript and protein levels of the endogenous *Nkx2-5* allele in E10.5 embryos. Under normoxic conditions, transcript and protein levels were equal in *Nkx2-5*^{+/+} and *Nkx2-5*^{+/-} embryos, consistent with the fact that *Nkx2-5*^{+/-} embryos develop normally (Fig. 3, Fig. S3A). However, in embryos exposed to low oxygen, levels of transcript were significantly reduced in exposed *Nkx2-5*^{+/-} embryos compared with unexposed *Nkx2-5*^{+/-} and with all *Nkx2-5*^{+/+} embryos, and levels of protein were significantly reduced in exposed *Nkx2-5*^{+/-} embryos, regardless of heart morphology, compared with exposed *Nkx2-5*^{+/+} embryos (Fig. 3).

Embryonic myocardial apoptosis and proliferation are not affected following maternal low-oxygen exposure

To further investigate the origins of the heart dilation and embryonic lethality in some *Nkx2-5*^{+/-} embryos, we examined apoptosis and proliferation in the heart 1 day after low-oxygen exposure (E10.5). No apoptosis was detected by activated Caspase 3 staining in the SHF, OFT or myocardium of embryos of either genotype (data not shown), consistent with our previous studies (Shi et al., 2016). Phosphorylated histone H3-positive nuclei were quantified in the myocardium and the proliferative index was the same in unexposed embryos of either genotype and in exposed embryos of all genotypes (Fig. S4). Thus, low-oxygen exposure per se does not cause apoptosis or overtly affect proliferation in the embryonic heart.

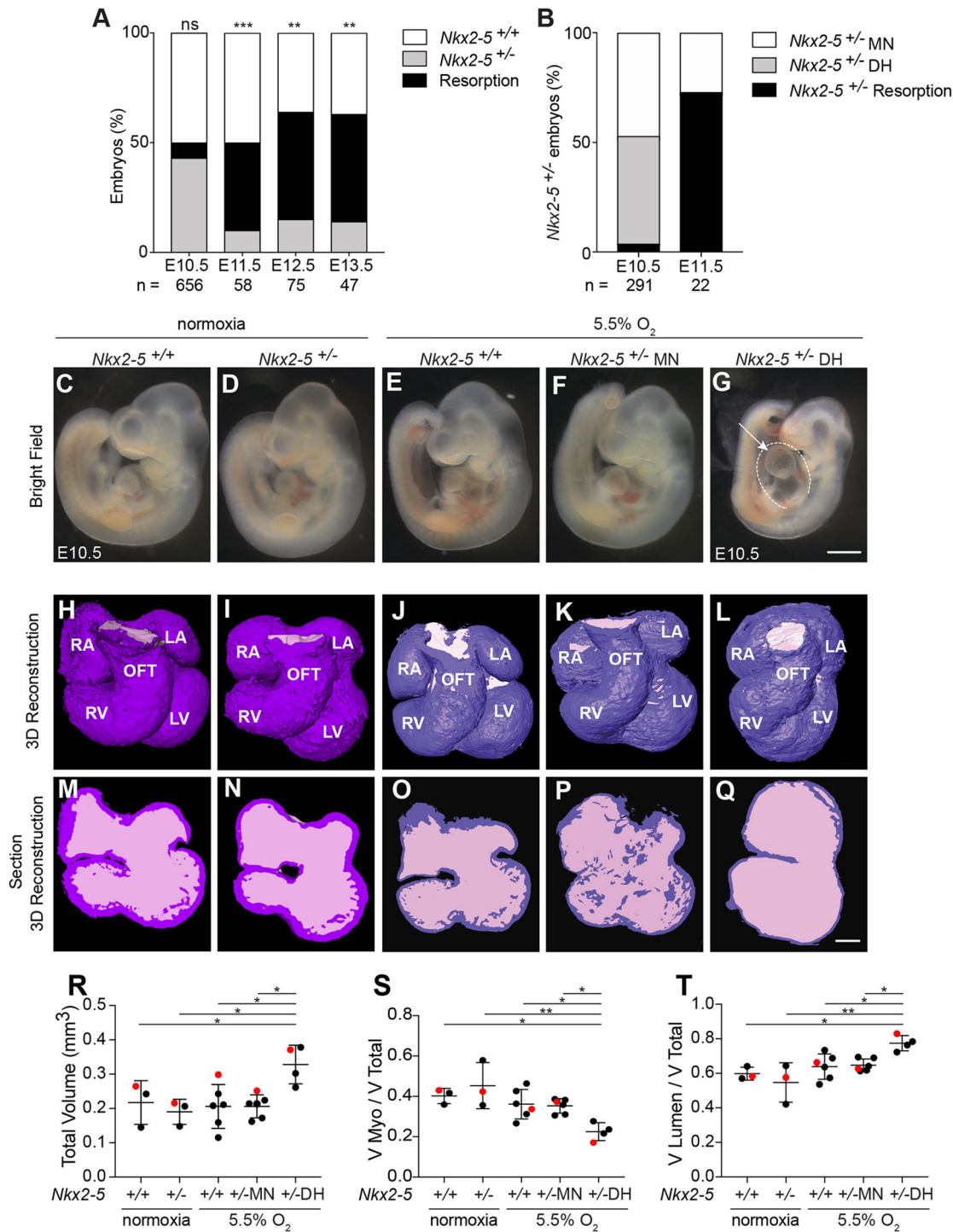


Fig. 2. Embryonic survival and heart morphology following maternal exposure to low oxygen. (A) Histograms showing the percentage of *Nkx2-5*^{+/+} (white), *Nkx2-5*^{+/-} (grey) embryos and resorptions (un-genotyped, black) at the indicated stages following 5.5% oxygen exposure at E9.5. For resorptions with genotypes, see Fig. S3. Significant deviation from the expected 1:1 Mendelian ratio in surviving embryos was calculated using chi-squared tests. (B) Histograms showing the percentage of *Nkx2-5*^{+/-} embryos displaying a morphologically normal heart (MN, white), a dilated heart (DH, grey) and exclusively *Nkx2-5*^{+/-} resorptions (black, see also Fig. S3) at the indicated stages. (C-G) Representative bright-field images of normoxic *Nkx2-5*^{+/+} and *Nkx2-5*^{+/-} E10.5 embryos (C, *n*=89; D, *n*=82), an *Nkx2-5*^{+/+} E10.5 embryo exposed to hypoxia (E, *n*=326), an *Nkx2-5*^{+/-} E10.5 embryo exposed to hypoxia with a morphologically normal heart (F, *n*=136), and an *Nkx2-5*^{+/-} E10.5 embryo exposed to hypoxia with a dilated heart (G, *n*=143, white arrow) with a pericardial effusion (dotted line). (H-L) Three-dimensional reconstructions of E10.5 hearts from a normoxic *Nkx2-5*^{+/+} embryo (H, *n*=3), a normoxic *Nkx2-5*^{+/-} embryo (I, *n*=3), a *Nkx2-5*^{+/+} embryo exposed to hypoxia (J, *n*=6), an *Nkx2-5*^{+/-} embryo exposed to hypoxia with a morphologically normal heart (K, *n*=6), and an *Nkx2-5*^{+/-} embryo exposed to hypoxia with a dilated heart (L, *n*=4). (M-Q) Frontal sections through three-dimensional reconstructions of the hearts shown in H-L, showing the chamber lumen (pink) and myocardium (purple). (R-T) Quantification of (R) total volume, (S) relative myocardial volume and (T) relative luminal volume of three-dimensional heart models. Red dots indicate quantification data from the images shown in H-L. Data were tested for statistical significance using one-way ANOVA with Tukey's post-hoc test. Data are mean±s.d. ns, not significant; **P*<0.05, ***P*<0.01, ****P*<0.001. RA, right atrium; LA, left atrium; RV, right ventricle; LV, left ventricle; OFT, outflow tract; DH, dilated heart; MN, morphologically normal heart. Scale bars: 1 mm in C-G; 100 μm in H-Q.

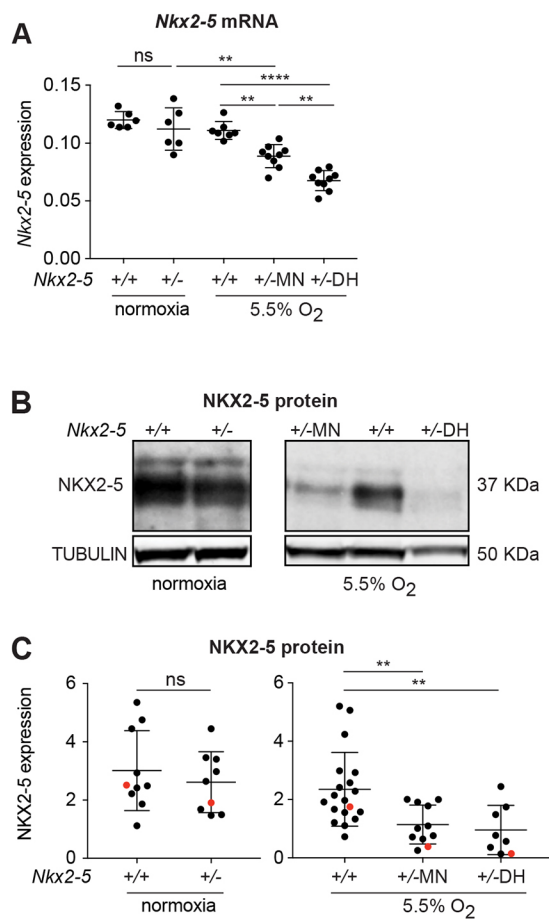


Fig. 3. Effects of maternal exposure to low oxygen on embryonic levels of *Nkx2-5* transcripts and protein. (A) Quantification of *Nkx2-5* transcript levels by qPCR relative to *Gapdh* and *Eef1e1* at E10.5. (B) Representative western blot showing NKX2-5 protein (37 kDa). (C) Quantification of NKX2-5 protein relative to tubulin. Red dots indicate quantification of the blots shown in B. Data were tested for statistical significance using one-way ANOVA with Tukey's post-hoc test. Data are mean±s.d. ns, not significant. ** $P < 0.01$, **** $P < 0.0001$. DH, dilated heart; MN, morphologically normal heart.

Chronotropy is affected in *Nkx2-5*^{+/-} embryos following maternal low-oxygen exposure

To investigate whether maternal low-oxygen exposure affects embryonic heart function, we performed *in utero* echocardiography on pregnant females at E10.5. In normoxia, embryonic heart rates

were >90 beats per minute (bpm), regardless of genotype (Fig. 4A,C; Fig. S5), consistent with previous reports (Corrigan et al., 2010; Mu and Adamson, 2006). By contrast, maternal low-oxygen exposure dramatically affected embryonic heart rates. Although 58% of the *Nkx2-5*^{+/+} embryos had a normal heart rate, 39% had a heart rate of 60-90 bpm and 3% had a heart rate under 60 bpm. This effect was exacerbated in *Nkx2-5*^{+/-} embryos in which 33% had a normal heart rate, 42% had a rate of 60-90 bpm and 25% had a rate under 60 bpm. By contrast, the heart rate of *Nkx2-5*^{+/-} embryos with dilated hearts were mostly less than 60 bpm (94%) (Fig. 4B,C; Fig. S5). Thus, embryonic cardiac function is impaired in all embryos, regardless of genotype, in response to maternal low-oxygen exposure. However, the *Nkx2-5*^{+/-} were more severely affected and are predicted to die based on their heart rates (Flores et al., 2014).

Molecular evidence for disrupted contractility in *Nkx2-5*^{+/-} embryos following maternal low-oxygen exposure

Nkx2-5 has a key role in development of both the cardiac conduction system and cardiac contractility (Jay et al., 2004; Risebro et al., 2012; Terada et al., 2011). *Nkx2-5* null embryos have reduced expression of *Myl2* (*Mlc2v*), a myosin expressed in the ventricular myocardium (Biben et al., 2000), and perinatal loss of *Nkx2-5* causes an enlarged heart with conduction and contractility defects (Briggs et al., 2008). Similar phenotypes, including a dilated heart and pericardial effusion, occur in embryos lacking expression of cardiac ion channels that are crucial for heart conduction (Weissgerber et al., 2006). Therefore, we tested the hypothesis that the cardiac conduction system might be perturbed in *Nkx2-5*^{+/-} embryos exposed to hypoxia. Transcript levels of genes involved in cardiac conduction were quantified in *Nkx2-5* embryonic hearts at E10.5, 1 day after maternal low-oxygen exposure (Fig. S6). There was no significant difference in expression of genes involved in the formation of the conduction system (Furtado et al., 2016; Mommersteeg et al., 2007), including *Hcn4*, *Gja5* (*Cx40*) and *Prox1*, a homeobox factor gene that plays a crucial role in maintaining muscle structure in the developing heart and is a direct upstream modifier of *Nkx2-5* (Risebro et al., 2012; Zhou et al., 2013). Similarly, no differences were found in the expression of the calcium channel genes *Cacnb2* and *Cacna1c*, the potassium channel gene *Kcnh2* or the sodium channel gene *Scn5a* (Fig. S6D-G). Likewise, no difference in expression levels was observed in the expression of the cardiac development marker genes *Gata4* or *Smad4* (Fig. S6K,L). It is noteworthy that gene expression levels are low (raw Ct >29) for *Gja5* (*Cx40*) and *Scn5a* in these embryos, making it difficult to draw robust conclusions at this stage.

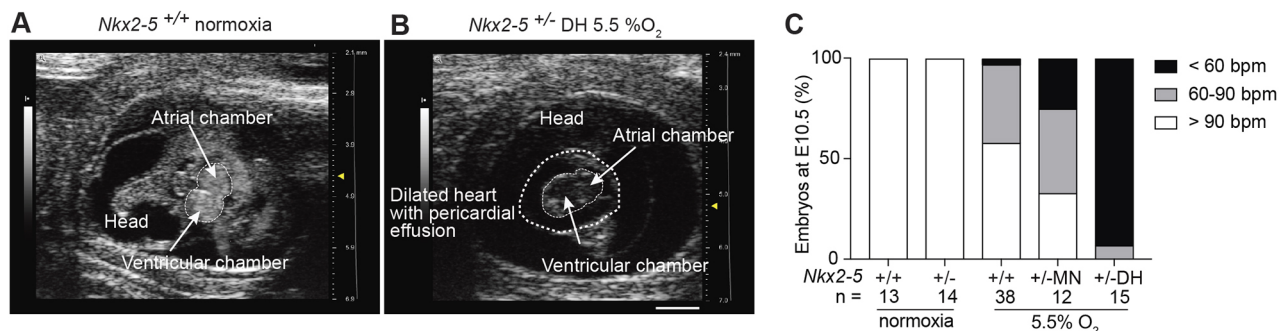


Fig. 4. *In utero* embryonic cardiac chronotropy assessment. (A,B) Representative *in utero* echocardiographic images of a control *Nkx2-5*^{+/+} E10.5 embryo presenting a normal heart (A, thin dotted line, $n = 13$) and a low-oxygen exposed *Nkx2-5*^{+/-} E10.5 embryo with a dilated heart (B, thin dotted line) with a pericardial effusion (B, thick dotted line, $n = 15$). (C) Histogram showing the percentage of E10.5 embryos displaying different heart rates in the given conditions. DH, dilated heart; MN, morphologically normal heart; bpm, beats per minute. Scale bar: 1 mm in A,B. See Fig. S5 for individual embryonic heart rates.

We also measured transcript levels in surviving embryos at E12.5. At this stage, all embryos were morphologically normal, regardless of genotype or exposure. No difference in expression was observed in *Nkx2-5^{+/+}* and *Nkx2-5^{+/-}* embryos at E12.5 for *Myl3*, *Myl2*, *Tnnt2*, *Nkx2-5*, *Hcn4*, *Cacnb2*, *Cacna1c*, *Kcnh2*, *Scn5a* (Fig. S7). By contrast, *Myl7* was increased independently of exposure in E12.5 *Nkx2-5^{+/-}* embryos compared with *Nkx2-5^{+/+}* embryos, indicating a genotype-specific effect (Fig. S7A). These results suggest that conduction defects or alteration in cardiac development gene expression are unlikely to cause the embryonic lethality observed in *Nkx2-5^{+/-}* embryos exposed to low oxygen.

We next explored the expression of genes involved in cardiac contraction at E10.5, 1 day after maternal low-oxygen exposure. No differences were observed in *Myh7* (*β-Mhc*), *Myl7* (*Mlc2a*) or *Myl3* (*Mlc1v*) (Fig. S6H-J) between *Nkx2-5^{+/+}* and *Nkx2-5^{+/-}* embryos. However, a significant decrease in *Actc1* was observed in *Nkx2-5^{+/-}* embryos with dilated hearts (Fig. 5A) compared with the *Nkx2-5^{+/+}* embryos. Given that the levels of *Actc1* were not significantly different between embryos in all other categories, the reduction in *Actc1* in *Nkx2-5^{+/-}* embryos with a dilated heart might be secondary to heart failure. Notably, we observed a decrease in *Myl2* (*Mlc2v*) and *Tnnt2* (*cTnT*) expression in all *Nkx2-5^{+/-}* embryos following maternal low-oxygen exposure, regardless of heart phenotype, compared with *Nkx2-5^{+/+}* embryos (Fig. 5B,C). Importantly, levels were the same in *Nkx2-5^{+/+}* and *Nkx2-5^{+/-}* embryos developed in normoxia, showing that genotype alone had no effect. Reduced *Myl2* and *Tnnt2* expression also occurred in *Nkx2-5^{+/-}* embryos with morphologically normal hearts, indicating that it is a primary effect of interaction between genetic predisposition and maternal low-oxygen exposure. Taken together these data suggest that GxE might directly or indirectly reduce expression of some genes encoding sarcomeric proteins of the cardiomyocyte.

Variability in embryonic heart morphology of *Nkx2-5^{+/-}* embryos is associated with the extent of HIF1α nuclear expression following maternal low-oxygen exposure

To further understand the interaction between low-oxygen exposure and *Nkx2-5* expression, we examined the timing of the appearance of the dilated heart phenotype by examining gross embryonic heart morphology at various stages after maternal low-oxygen exposure at E9.5, as outlined (Fig. 6A). Immediately after hypoxic exposure, embryo and heart morphology were normal, regardless of genotype (Fig. 6B,C). This was also true for up to 4 h after exposure (data not shown). However, by 5 h after exposure, 45% of the *Nkx2-5^{+/-}* embryos had a dilated heart (Fig. 6D-F). Stabilisation and nuclear

localisation of HIF1α occurs in hypoxic cells (Wang and Semenza, 1993). To address whether HIF1α has a role in heart dilation and embryo death following low-oxygen exposure, we quantified the levels of nuclear HIF1α in embryonic hearts immediately after or 5 h after low-oxygen exposure. There was no difference in levels of nuclear HIF1α in the myocardium of *Nkx2-5^{+/+}* and *Nkx2-5^{+/-}* embryos immediately after exposure (Fig. 6G-I). By contrast, 5 h after exposure, *Nkx2-5^{+/-}* hearts showed significantly higher levels of nuclear HIF1α compared with *Nkx2-5^{+/+}* hearts (Fig. 6J-L). As expected, the levels of *Hif1α* mRNA were unchanged by hypoxia in *Nkx2-5^{+/-}* embryos, suggesting that HIF1α protein was stabilised (Fig. S6M). Thus, the cardiac dilation and lethality of *Nkx2-5^{+/-}* embryos caused by maternal low-oxygen exposure may be due to aberrantly prolonged stabilisation of HIF1α.

Chemical stabilisation of HIF1α induces a heart phenotype, as observed in embryos following maternal low-oxygen exposure

To investigate whether prolonged HIF1α stabilisation following low-oxygen exposure leads to impaired heart function and death, we used cobalt chloride (CoCl₂) treatment to stabilise HIF1α in normoxia (Wang and Semenza, 1993). Pregnant mice were injected with CoCl₂ at E9.5, then injected with Hypoxyprobe after 5 h, and embryos were harvested 3 h later (Fig. S8A). Hypoxyprobe identifies cells with 2% oxygen or less (Raleigh et al., 1999). Maternal injection of 40 mg/kg CoCl₂ was sufficient to increase HIF1α protein levels in mouse embryos without reducing cellular oxygen levels below physiological levels observed at normoxia (Fig. S8B). This dose induced HIF1α nuclear expression in the myocardium similar to maternal exposure to 5.5% oxygen for 8 h (Fig. S8C-E). We next injected CoCl₂ into pregnant mice at E9.5, and harvested embryos after 8 h. All embryos were morphologically normal and HIF1α was elevated to equivalent levels in the myocardium of *Nkx2-5^{+/+}* and *Nkx2-5^{+/-}* embryos (Fig. 7B-J). This was also the case for embryos harvested 13 h after CoCl₂ injection (Fig. 7K-S). However, 24 h after CoCl₂ injection (E10.5), all embryos, regardless of genotype, had pericardial effusion and altered hearts, as judged by light microscopy (Fig. 7T-X). Thus, aberrantly prolonged nuclear expression of HIF1α in the absence of low-oxygen exposure at E9.5 is sufficient to induce a heart phenotype. To further address the mechanism, we quantified *Nkx2-5* mRNA and protein levels in these embryos. Reduced *Nkx2-5* mRNA and protein levels were observed in embryos exposed to CoCl₂ *in utero* compared with water controls, regardless of genotype (Fig. 8A-C). Taken together, these data indicate that

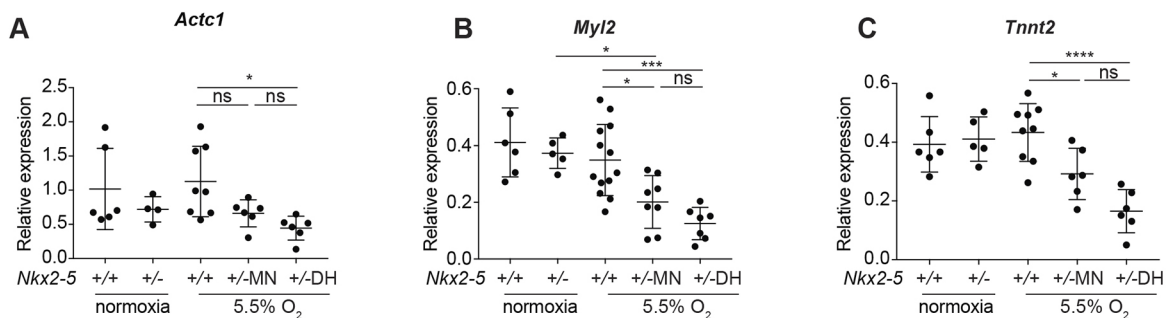
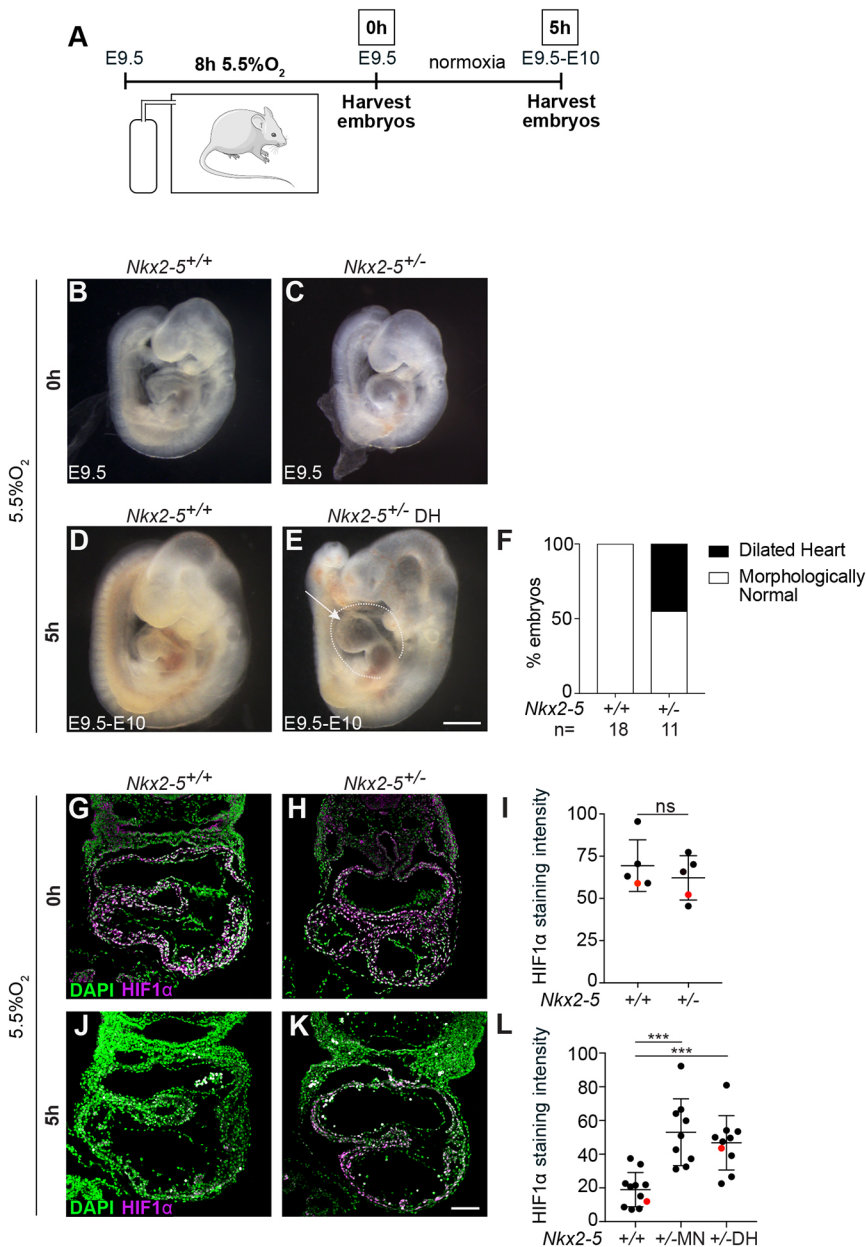


Fig. 5. Effects of maternal exposure to low oxygen on embryonic levels of cardiac contractility gene transcripts at E10.5. (A-C) Quantification of transcript levels of (A) *Actc1*, (B) *Myl2* and (C) *Tnnt2* at E10.5 by qPCR relative to *Gapdh* and *Eef1e1*. Data were tested for statistical significance using one-way ANOVA with Tukey's post-hoc test. Data are mean±s.d. **P*<0.05, ****P*<0.001, *****P*<0.0001. ns, not significant. DH, dilated heart; MN, morphologically normal heart.



perdurance of nuclear HIF1α is responsible for loss of *Nkx2-5* mRNA and protein, consequent pericardial effusion and altered heart morphology.

DISCUSSION

Mouse heart development occurs over a protracted period of time, first evident with appearance of the cardiac crescent at E8 and largely ceasing at E15 when the heart reaches its final four-chambered form (de Boer et al., 2012). At E9.5, the mouse heart is undergoing considerable morphogenetic change and contraction of the myocardium is required to circulate blood throughout the embryo, yolk sac and placenta (Andrés-Delgado and Mercader, 2016). At this time, exposure of the embryo to 5.5% oxygen increases cellular hypoxia in embryos, above physiological levels, and leads to stabilisation of HIF1α (O'Reilly et al., 2014; Shi et al., 2016). Nuclear HIF1α is predominantly in the myocardium, likely due to the relatively high energy requirements of the contracting sarcomeres/myocardium. In wild-type mouse embryos, we find that

HIF1α is observed in the myocardium immediately after the 8 h at 5.5% oxygen exposure and levels are reduced to background levels 5 h later (Table S3). Embryonic heart rates are also reduced at E10.5 and presumably are rectified to sufficiently meet the demands of the rapidly growing embryos, as about 90% of these are viable at E17.5 (Shi et al., 2016). Although almost all embryos are viable at E17.5, about 50% present with heart defects (VSD, OA, DORV, TGA, ASD), consistent with disruption of FGF signalling in the SHF. The effects of exposure to less extreme levels of lowered oxygen are not as great, but are also less studied (O'Reilly et al., 2014; Shi et al., 2016). After 3 h of exposure to 8% or 9% oxygen, embryonic cellular hypoxia is increased. Eight hours after exposure to 8% oxygen, HIF1α is stabilised in the myocardium and FGF signalling is reduced by about 30%, with 0-12.5% heart defects (VSD, muscular VSD and OA) observed at E17.5 (O'Reilly et al., 2014). It is not possible to compare directly the levels of low-oxygen exposure in mice with humans in a meaningful way. Nevertheless, these studies indicate that low oxygen is a credible

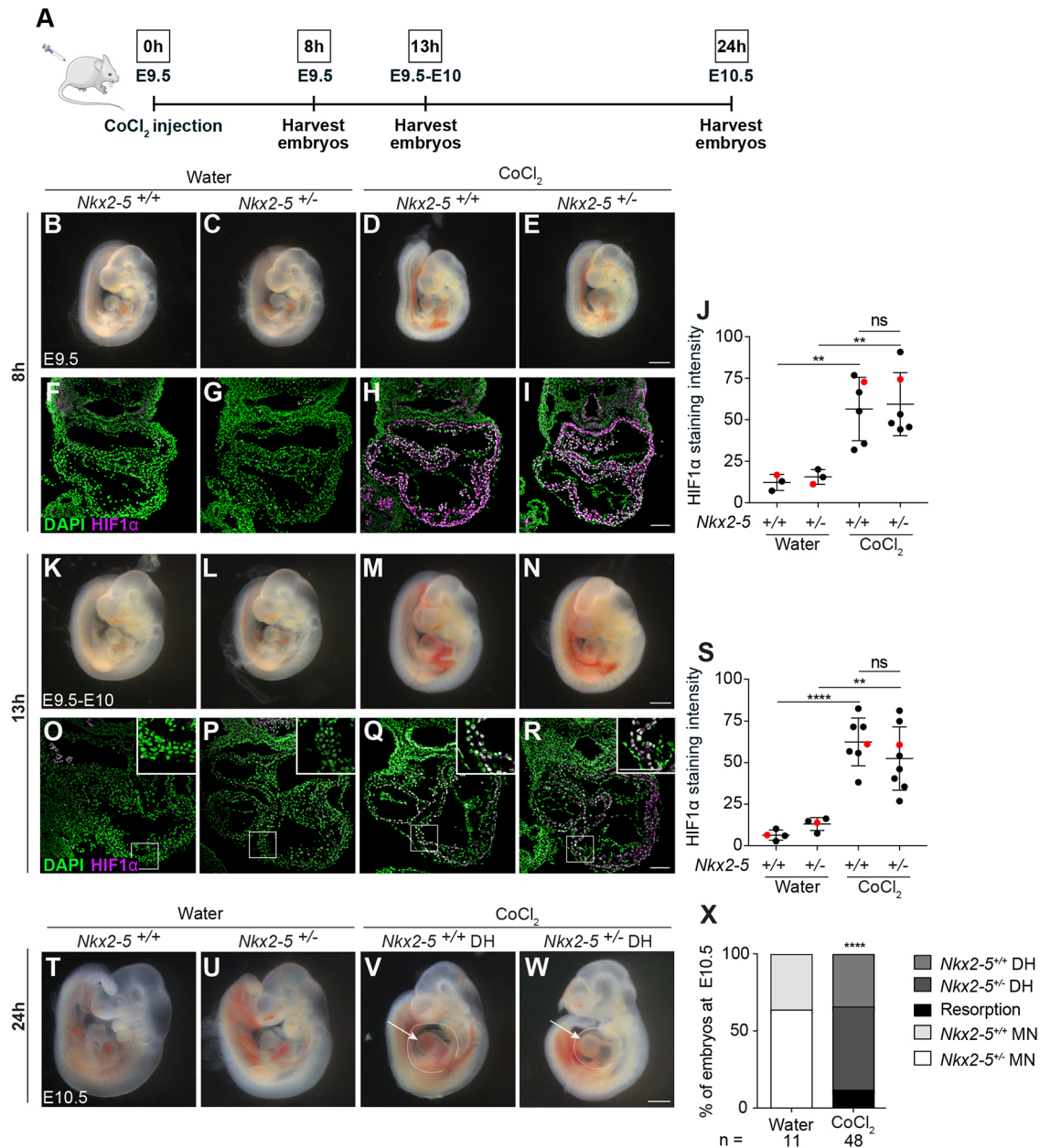


Fig. 7. Alterations in heart morphology and HIF1 α accumulation are apparent after maternal cobalt chloride exposure. (A) Schematic diagram illustrating the experimental design. Pregnant females were injected with 40 mg/kg of cobalt chloride at E9.5 (0 h), and embryos harvested 8, 13 or 24 h later. (B-E) Representative bright-field pictures of *Nkx2-5*^{+/+} (B, n=9), *Nkx2-5*^{+/-} control embryos (C, n=8), *Nkx2-5*^{+/+} (D, n=8) and *Nkx2-5*^{+/-} (E, n=9) embryos 8 h after maternal injection of cobalt chloride. (F-I) Comparison of expression levels of HIF1 α (magenta) in control *Nkx2-5*^{+/+} (F, n=7), *Nkx2-5*^{+/-} (G, n=6) embryos, and injected *Nkx2-5*^{+/+} (H, n=6) and *Nkx2-5*^{+/-} (I, n=6) embryos 8 h after maternal injection of cobalt chloride. Nuclei are stained with DAPI (green). (J) Quantification of HIF1 α staining intensity. Red dots indicate quantification of the embryos shown in F-I. (K-N) Representative bright-field pictures of *Nkx2-5*^{+/+} (K, n=3), *Nkx2-5*^{+/-} control embryos (L, n=4), and *Nkx2-5*^{+/+} (M, n=6) and *Nkx2-5*^{+/-} (N, n=13) embryos 13 h after maternal cobalt chloride injection. (O-R) Comparison of expression levels of HIF1 α (magenta) in control *Nkx2-5*^{+/+} (O, n=3), *Nkx2-5*^{+/-} (P, n=4), *Nkx2-5*^{+/+} (Q, n=7) and *Nkx2-5*^{+/-} (R, n=8) embryos 13 h after cobalt chloride exposure. Nuclei are stained with DAPI (green). Insets in O-R are higher magnifications of the boxed areas. (S) Quantification of HIF1 α protein levels. Red dots indicate quantification of the embryos shown in O-R. (T-W) Representative bright-field pictures of *Nkx2-5*^{+/+} (T, n=5), *Nkx2-5*^{+/-} control embryos (U, n=6), *Nkx2-5*^{+/+} (V, n=17) and *Nkx2-5*^{+/-} (W, n=27) embryos 24 h after maternal injection of cobalt chloride. Dilated hearts (white arrows) with pericardial effusion (dotted line). (X) Histogram showing the percentage of heart defects present in E10.5 embryos following water or cobalt chloride injection. Data were tested for statistical significance using one way ANOVA with Tukey's post-hoc test (J,S) or chi-squared test (X). Data are mean \pm s.d. ns, not significant. ***P*<0.01, *****P*<0.0001. DH, dilated heart; MN, morphologically normal heart. Scale bars: 1 mm in B-E,K-N,T-W; 100 μ m in F-I,O-R.

cause of variable penetrance and expressivity of heart defects in humans.

Here, we report that a combination of genetic susceptibility and maternal hypoxia leads to increased penetrance and expressivity of heart defects in mice. We show that GxE variably affects heart

morphology, depending on the genetic background (with regard to FGF signalling or cardiac transcription factors) and the level of oxygen deprivation. Exposure to 8% oxygen does not induce GxE in wild-type embryos or in embryos heterozygous null for *Fgf8*, *Fgf1* or *Fgf2*, with only low incidence of heart defects observed.

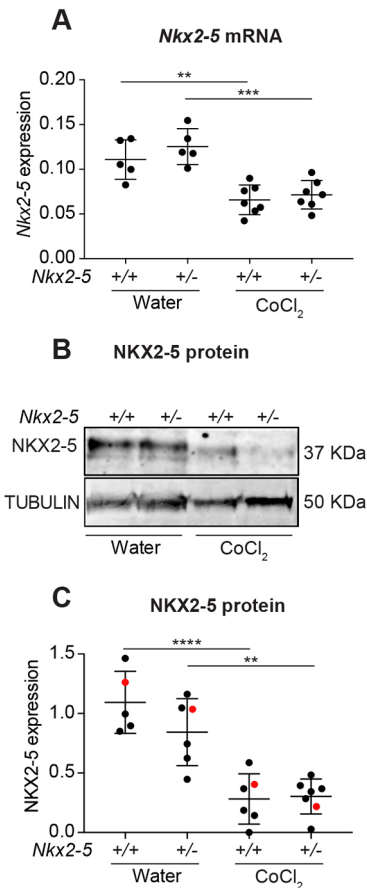


Fig. 8. Molecular response to chemical accumulation of HIF1 α on *Nkx2-5* at E10.5. (A) Quantification of *Nkx2-5* transcript levels by qPCR relative to *Gapdh* and *Eef1e1* at E10.5. (B) Representative western blot showing NKX2-5 protein (37 kDa). (C) Quantification of NKX2-5 protein relative to tubulin. Red dots indicate quantification of the images shown in B. Data were tested for statistical significance using one-way ANOVA with Tukey's post-hoc test. Data are mean \pm s.d. ** P <0.01, *** P <0.001, **** P <0.0001.

Embryos heterozygous for both *Fgfr1* and *Fgfr2* exhibit GxE with 8% oxygen exposure, consistent with the fact that these genes show genetic redundancy in the developing heart and somites (Park et al., 2008), providing further support to the concept that FGF signalling has a dose-dependent effect on embryogenesis (Naiche et al., 2011).

Exposure to 8% oxygen did not increase the incidence of heart defects in *Tbx5*, *Tbx1* or *Nkx2-5* heterozygous null embryos compared with non-exposed controls. It is unclear why heterozygosity for these genes does not interact with 8% oxygen. We have shown that 8% oxygen interacts with heterozygosity in Notch pathway genes to disrupt somitogenesis (Sparrow et al., 2012). In this case, hypoxia inhibits FGF signalling, which disrupts Notch signalling in the presomitic mesoderm, leading to somite and vertebral defects. Hypoxia also inhibits FGF signalling in the SHF and disrupts heart development (Shi et al., 2016). The lack of GxE here might indicate that these transcription factors are not associated with FGF signalling. Evidence of an association could only be found with *Tbx1*, with expression of *Fgf8* partially rescuing heart defects induced by loss of *Tbx1* in mice (Vitelli et al., 2010, 2002). Hypoxia also stabilises HIF1 α in cardiomyocytes and there is evidence to indicate that HIF1 α positively and/or negatively regulates the expression of cardiac transcription factor genes, including *Tbx5* and *Nkx2-5* (Bohuslavova et al., 2013; Krishnan

et al., 2008; Nagao et al., 2008). Despite some evidence linking these transcription factors to FGF signalling or HIF1 α , it is not clear why GxE between these genes and 8% oxygen was not observed in the context of heart development. Similar variable results have been reported where hypoxia exposure of mice heterozygous for genes that are crucial for somitogenesis did not always result in GxE (Sparrow et al., 2012, 2011).

More extreme low-oxygen exposure of 5.5% induces an interaction in embryos heterozygous for *Tbx1* or *Nkx2-5*. With respect to *Tbx1*, the incidence of heart defects is increased, whereas the GxE observed with *Nkx2-5* causes a more-extreme phenotype of death *in utero*. This variability seen in the ability of GxE to disrupt heart development might be due to many factors, including: genetic or functional redundancy; the function of the gene in heart development; distinct susceptibility of gene expression and the function of the gene product to the oxygen levels; and the duration of the exposure and/or the timing of the exposure with respect to the timing of gene function.

The observed GxE between *Nkx2-5* and 5.5% oxygen rapidly affected heart function and embryo survival (Table S3). Tracking this demise provides insight into the natural history of this heart failure and its molecular triggers. The first sign of the impact that hypoxia has on the heart is at 5 h after exposure, when half the embryos have a dilated heart and elevated expression of HIF1 α in the myocardium (Table S3). The incidence of dilated hearts is unchanged at E10.5 following hypoxic exposure, indicating that these embryos still have dilated hearts 16 h later (Table S3). At this stage, we find that dilated hearts exhibit impaired contractility, hallmarks of which are also present in the normal, non-dilated, hearts (Table S3). Specifically, the heart rate is reduced in *Nkx2.5*^{+/-} embryos with normal hearts and more so in those with dilated hearts (Table S3). The same trend is evident with reduced expression of two genes (*Myl2* and *Tnnt2*), which encode contractile proteins in the sarcomere (Table S3). Just 1 day later at E11.5, 80% of the *Nkx2.5*^{+/-} embryos have died, including all those with dilated hearts and some with normal hearts (Table S3). Surviving *Nkx2.5*^{+/-} embryos at E12.5 show normal expression of genes encoding protein components of the conduction and contractile systems (Table S3). Thus, it is possible that reduced expression of the sarcomeric proteins in normal hearts at E10.5 may be a trigger of cardiac dilation and embryo death by the next day.

HIF1 α is stabilised in the nucleus when cellular oxygen levels drop below a threshold (half maximal response 1.5–2.0% oxygen; Jiang et al., 1996) and, accordingly, HIF1 α is elevated in the embryonic myocardium following gestational hypoxia, independent of genotype (Table S3; O'Reilly et al., 2014; Shi et al., 2016). HIF1 α levels are not sustained in *Nkx2.5*^{+/-} embryos upon return to normoxia. Sustained HIF1 α protein levels and reduced *Nkx2-5* expression in *Nkx2-5*^{+/-} embryos may trigger heart failure by E11.5. Our findings are supported by the observation that embryos with elevated HIF1 α levels throughout the *Nkx2-5* cell lineage have ventricular wall thinning and chamber dilation, phenotypes that we also observed in the *Nkx2-5*^{+/-} embryos exposed to hypoxia (Menendez-Montes et al., 2016).

There is some conflicting evidence that HIF1 α might regulate *Nkx2-5* expression (Bohuslavova et al., 2013; Nagao et al., 2008). However, our finding that elevated HIF1 α levels, either by exposure to low oxygen or to CoCl₂, reduced NKX2-5 expression is consistent with one study that shows decreased NKX2-5 expression in the myocardium of embryos from females exposed to 14% oxygen for 8 days between E10.5 and E18.5 (Moumne et al., 2018). There is also clear evidence that mouse heart development is

dependent on NKX2-5 in a dose-dependent manner and that *Nkx2-5* is required not only early in development for correct cardiac morphology but also later on, in the establishment and function of the conduction system and for cardiac contractility (Prall et al., 2007). Thus, in the context of our study, hypoxia may cause NKX2-5 levels to fall below a threshold, precipitating a reduction in contractility for a period of time extending beyond the effects of the low-oxygen exposure. Reduced contractility would further limit circulation and oxygen delivery, exacerbating cellular hypoxia. It is possible that this cycle in *Nkx2.5*^{+/-} embryos leads to rapid heart failure and embryo death. We find that the expression of some contractile protein genes (*Myl2* and *Tnnt2*) is reduced in hypoxia-exposed *Nkx2.5*^{+/-} embryos at E10.5. Loss-of-function mutations in these genes results in heart failure and death by E10 to E12.5 (Chen et al., 1998). By contrast, we observe no difference in expression of ion channel genes at E10.5. This indicates that hypoxia does not directly affect the conduction system and/or that E10.5 is too early, as the sinoatrial node is not morphologically distinct until E11.5 (van Weerd and Christoffels, 2016).

In this study, CoCl₂ prolongs elevated HIF1 α protein levels in the myocardium, and hearts of embryos exposed to CoCl₂ appeared dilated with pericardial effusion. This suggests that sustained HIF1 α in low-oxygen exposed *Nkx2.5*^{+/-} embryos is, at least in part, responsible for the observed heart phenotype. This is in keeping with another study reporting that a single maternal injection of 30 mg/kg CoCl₂ 2 days earlier, at E7.5, also perturbs heart development and expression of *Nkx2.5* (Yuan et al., 2017). Variability in CoCl₂ dose, the timing of injection, the stage of analysis and the mouse strain may explain differences observed between the two studies. Further work is required to determine whether reduced expression of the contractile protein genes is due to hypoxia, to sustained HIF1 α or to reduced *Nkx2-5* expression.

Variable penetrance and expressivity of phenotype has been reported among related and unrelated individuals that carry the same pathogenic variant of *NKX2-5* (Benson et al., 1999, four different alleles; McElhinney et al., 2003, Arg25Cys variant). This may be the result of modifier genes or due to the influence of non-genetic factors. Our data support a role for environmental factors in this variability. The timing, extent and nature of an environmental ‘second hit’ in combination with specific genetic predisposition are all likely to influence the phenotype. Other plausible environmental factors include maternal age (Schulkey et al., 2015), diet (Shi et al., 2017), illness ((Wren et al., 2003)), infections (Dewan and Gupta, 2012) or teratogen exposure (Kopf and Walker, 2009). Finally, our results suggest that a relatively short period of hypoxia, coupled with a genetic predisposition, can result in embryonic death. Therefore, it is possible that families carrying a pathogenic *NKX2-5* allele may also have a higher rate of miscarriages.

In conclusion, we demonstrate that interaction between genetic predisposition to heart defects and an environmental factor causes heart defects and embryo loss in mice. These findings indicate that some cases of foetal death and/or congenital heart disease might arise by such an interaction in humans. Our findings also provide insights into the molecular mechanisms underlying the interaction between genetic predisposition and factors that can cause embryonic cellular hypoxia. Thus, they are relevant to understanding the sporadic nature of congenital heart disease and are important for framing the information given during genetic counselling in such a context of sporadic defects. They might also inform discussion concerning guidelines associated with pregnancy management.

MATERIALS AND METHODS

Mouse lines

This research was performed following the guidelines, and with the approval, of the Garvan Institute of Medical Research/St. Vincent’s Animal Experimentation Ethics Committee (research approvals 9/33, 12/33, 15/27 and 18/27). Mouse lines used in these studies were as follows: *Fgf8* [*Fgf8*^{tm2Moon}] (Park et al., 2006); *Fgfr1* [*Fgfr1*^{tm5.1Sor}] (Hoch, 2006); *Fgfr2* [*Fgfr2*^{tm1Dor}] (Yu et al., 2003); *Tbx1* [*Tbx1*^{tm1Bld}] (Lindsay et al., 2001); *Tbx5* [*Tbx5*^{tm1Jse}] (Bruneau et al., 2001); and *Nkx2-5* [*Nkx2-5*^{tm4Rph}] (Biben et al., 2000).

Male mice heterozygous for the gene of interest were crossed with 8- to 18-week-old C57BL/6J wild-type females to produce heterozygous and wild-type embryos. Double heterozygous *Fgfr1/Fgfr2* embryos were produced by crossing *Fgfr1*^{+/-}; *Fgfr2*^{+/-} males with C57BL/6J females. Pregnant mice were exposed to reduced oxygen levels at normal atmospheric pressure as described previously (Sparrow et al., 2012). After exposure, the mice were either sacrificed immediately and embryos harvested, or mice were returned to normoxia for embryo harvest at a later date. For cobalt chloride experiments, pregnant mice were dosed with 40 mg/kg dissolved in water by a single intraperitoneal injection at E9.5. Hypoxyprom experiments were performed as described previously (O’Reilly et al., 2014).

Heart morphology analysis

Heart morphology was examined using optical projection tomography (OPT) according to Shi et al. (2016). For analysis of E10.5 hearts, embryo torsos were immunostained with anti-smooth muscle actin (SMA, Table S5) in whole mount (Chapman et al., 2011), dehydrated in methanol and cleared for at least 10 min in 1:2 benzoic acid/benzyl benzoate (BABB). These were superglued directly to the mounting post of the OPT scanner. For whole E17.5 hearts, hearts were dissected and fixed overnight in 3% glutaraldehyde, dehydrated in methanol and cleared in BABB for at least 24 h. OPT scanning was performed at a resolution of 3.2 μ m, as described by Shi et al. (2016). For myocardial and luminal volume quantification of the E10.5 hearts, SMA staining was used to separate the myocardium from the lumen on Amira software as described by (del Monte-Nieto et al. (2018).

Ultrasound assessment of the embryonic heart

Pregnant mice were anaesthetised using 5% isoflurane in medical oxygen and transferred to the Vevo Integrated Animal Platform that includes a warming pad with a nosecone, integrated ECG recording electrodes of the high frequency echocardiography machine (Vevo 2100, FujiFilm Visualsonics). The chest and abdomen were shaved, washed with water and ultrasound gel applied, which was also used to electrically connect the feet to their respective ECG electrodes. During scanning, isoflurane dose was reduced to 1-2% to maintain maternal heart and respiratory rates at over 450 beats per minute (bpm) and over 120 breaths per minute throughout the examination, while maintaining immobility. The maternal cardiac dimension from long axis and short axis B-mode was determined using a MS400 probe ($n=23$ females), and the embryos on the right and left uterine horns were located and counted. The embryos were then examined using a MS700 probe by rotating the probe to align the spinal somites and head in the B-mode field of view. Colour Doppler scanning was used to aid identification of the arterial outflow and atrioventricular tracts from which Doppler data were recorded for heart rate determination. Only the most superficial embryos could be imaged (an average of four per litter) because the other embryos were too deep. After imaging, the females were sacrificed and embryos collected, taking care to identify which embryos had been imaged. Heart rates values were calculated from Doppler data using Vevo 2100 software in a blinded manner by two independent researchers.

Immunohistochemistry

For immunohistochemistry of sections, embryos were harvested at different time points (E9.5-E10.5), fixed overnight in 4% paraformaldehyde at 4°C, paraffin embedded and sectioned in the transverse plane at 10 μ m. To minimise inter-slide staining variation, tissue arrays were made by putting six sections from each heart of two to four embryos on a single slide. Antigen retrieval for all antibodies was carried out using TE buffer (Moreau

et al., 2014). The antibodies used are listed in Table S5. Finally, slides were mounted in Mowiol with DABCO (Moreau et al., 2014). Images were captured on a LSM 710 upright confocal microscope (Carl Zeiss). For detecting HIF1 α in paraffin sections, biotinylated donkey anti-rabbit secondary and streptavidin Cy3 tertiary reagents were used (Table S5).

Western blot

Proteins were extracted from isolated E10.5 hearts in RIPA buffer [150 mM NaCl, 1% IGEPAL CA-630, 0.5% sodium deoxycholate, 0.1% SDS, 50 mM Tris (pH 8)]. Protein (50 μ g) was loaded on a 4-12% Bis-Tris Plus Gel using a mini Bolt system (Life Technologies) and transferred using the mini Bolt system to a nitrocellulose membrane (0.45 μ m pore size, Amersham) according to the manufacturer's instructions. For NKX2-5, protein detection was performed using WesternBreeze (ThermoFisher Scientific) according to the manufacturer's instructions. The antibodies used are listed in Table S5.

Isolation of RNA and RT-qPCR

Embryonic hearts were collected, snap frozen in liquid nitrogen and stored at -80°C . Total RNA was isolated using TriReagent (Life Technologies) following the manufacturer's protocol. The tissues were homogenised using an insulin syringe. RNA purity (A_{260}/A_{280} ratio ≥ 1.8) and concentration were measured using the NanoDrop ND-1000 Spectrophotometer. Total RNA (1000 ng) was converted into cDNA in a total volume of 20 μ l using QuantiTect Reverse Transcription Kit following the manufacturer's instructions. The qPCR reaction contained 4 ng of cDNA. The qPCR reactions contained LightCycler 480 SYBR Green I Master (Roche) and the forward and reverse primer, each at a final concentration of 0.3 μ M. Each sample was analysed in triplicate. The amplification protocol consisted of 10 min at 95°C followed by 45 cycles of 95°C for 15 s and 60°C for 30 s, completed with a standard melting curve protocol. Melting curve analysis (LightCycler480, Roche) and quantifications were performed using the Lightcycler 480 software (Roche). Eight reference genes were selected from Ruiz-Villalba et al. (2017) and the two best ones were selected with NormFinder and used as housekeeping genes. Each pair of primers, listed in Table S4, was validated on mouse embryonic cDNA for specificity (one peak on the melting curve), efficiency (>-3.6) and error (<0.2). Raw values were exported from Microsoft Excel and relative expression calculated using the $2^{-\Delta\Delta\text{Ct}}$ formula.

Quantification

Staining intensity of immunohistochemistry on paraffin sections was quantified using ImageJ 1.48a (NIH). Briefly, LSM files generated by confocal microscopy were imported into ImageJ. The region of interest (ROI) was manually defined, and the image was thresholded for both the staining of interest and nuclei. Identical thresholding values were used for all images of each experiment. The signal of the protein of interest above threshold was quantified as a raw integrated density and divided by the nuclei area. For proliferation measurement, the percentage of phospho-histone H3 positive cells in each embryo was calculated as the ratio of total number of phospho-histone H3-positive cells against the total number of To-Pro3+ nuclei from five to six independent sections from the same embryo. Western blots analysed by chemiluminescence were digitised using a FLA-5100 scanner (Fujifilm) and converted to TIFF format using ImageJ. Western blots analysed by Odyssey Imager (LI-COR) were scanned at high resolution and saved as TIFF files. In both cases, bands were quantitated using Gelanalyzr (gelanalyzr.com).

Statistical analyses

All statistical analyses were performed with Prism 7 (GraphPad Software). Data from immunohistochemistry, western blots and qPCRs were first tested for normal distribution using either the d'Agostino and Pearson normality test (when $n > 8$) or the Shapiro-Wilk normality test (when $n < 8$). All datasets were normally distributed. Therefore, all datasets were tested for statistical significance using an ordinary one-way ANOVA with Tukey's post-hoc test or Student's *t*-test. The statistical significance of the incidence of heart defects or resorbed embryos in exposed versus unexposed embryos (Fig. 1,

Fig. S2) was tested using a two-tailed Fisher's exact test. Chi-squared test were used to test for divergence from expected Mendelian ratios (Figs 1 and 7). In all the figures, data are mean \pm s.d.

Acknowledgements

The authors thank the following for generously providing mice used in this study: Benoit Bruneau (Tbx5tm1Jse); David Ornitz and Washington University (Fgfr2tm1Dor/J); and Philippe Soriano (B6.129S4-Fgfr1tm5.1Sor/J) and the Jackson Laboratory. The authors thank BioCORE staff for technical assistance.

Competing interests

The authors declare no competing or financial interests.

Author contributions

Conceptualization: S.L.D.; Methodology: J.L.M.M., D.B.S., G.C., S.L.D.; Validation: J.L.M.M., D.B.S., G.C., S.L.D.; Formal analysis: J.L.M.M., D.B.S., G.C., S.L.D.; Investigation: J.L.M.M., S.K., E.M.M.A.M., K.S.L., M.X.Y., V.C.O., D.B.S., G.C.; Resources: A.B., A.M.M., R.P.H.; Data curation: J.L.M.M., D.B.S., G.C.; Writing - original draft: J.L.M.M., G.d.M.-N., G.C., S.L.D.; Writing - review & editing: J.L.M.M., E.M.M.A.M., G.d.M.-N., A.B., M.P.F., A.M.M., R.P.H., D.B.S., G.C., S.L.D.; Visualization: J.L.M.M., D.B.S., G.C., S.L.D.; Supervision: J.L.M.M., D.B.S., G.C., S.L.D.; Project administration: S.L.D.; Funding acquisition: D.B.S., G.C., S.L.D.

Funding

This work was supported by the National Health and Medical Research Council (NHMRC) (fellowships ID1135886 and ID1042002 to S.L.D., ID573732 to R.P.H., project grant ID1019776 to S.L.D. and D.B.S., and program grant ID1074386 to R.P.H. and S.L.D.), by the British Heart Foundation (RE/13/1/30181 and FS/17/55/33100 to D.B.S.), by the Office of Health and Medical Research NSW Government (to S.L.D., R.P.H.); and by Chain Reaction (The Ultimate Corporate Bike Challenge) (to S.L.D.).

Supplementary information

Supplementary information available online at <http://dev.biologists.org/lookup/doi/10.1242/dev.172957.supplemental>

References

- Andrés-Delgado, L. and Mercader, N. (2016). Interplay between cardiac function and heart development. *Biochim. Biophys. Acta* **1863**, 1707-1716.
- Benson, D. W. (2010). Genetic origins of pediatric heart disease. *Pediatr. Cardiol.* **31**, 422-429.
- Benson, D. W., Silberbach, G. M., Kavanaugh-McHugh, A., Cottrill, C., Zhang, Y., Riggs, S., Smalls, O., Johnson, M. C., Watson, M. S., Seidman, J. G. et al. (1999). Mutations in the cardiac transcription factor NKX2.5 affect diverse cardiac developmental pathways. *J. Clin. Invest.* **104**, 1567-1573.
- Biben, C., Weber, R., Kesteven, S., Stanley, E., McDonald, L., Elliott, D. A., Barnett, L., Köentgen, F., Robb, L., Feneley, M. et al. (2000). Cardiac septal and valvular dysmorphogenesis in mice heterozygous for mutations in the homeobox gene *Nkx2-5*. *Circ. Res.* **87**, 888-895.
- Blue, G. M., Kirk, E. P., Sholler, G. F., Harvey, R. P. and Winlaw, D. S. (2012). Congenital heart disease: current knowledge about causes and inheritance. *Med. J. Aust.* **197**, 155-159.
- Bohuslavova, R., Skvorova, L., Sedmera, D., Semenza, G. L. and Pavlinkova, G. (2013). Increased susceptibility of HIF-1 α heterozygous-null mice to cardiovascular malformations associated with maternal diabetes. *J. Mol. Cell. Cardiol.* **60**, 129-141.
- Briggs, L. E., Takeda, M., Cuadra, A. E., Wakimoto, H., Marks, M. H., Walker, A. J., Seki, T., Oh, S. P., Lu, J. T., Summers, C. et al. (2008). Perinatal loss of *Nkx2-5* results in rapid conduction and contraction defects. *Circ. Res.* **103**, 580-590.
- Bruneau, B. G., Logan, M., Davis, N., Levi, T., Tabin, C. J., Seidman, J. G. and Seidman, C. E. (1999). Chamber-specific cardiac expression of *Tbx5* and heart defects in Holt-Oram syndrome. *Dev. Biol.* **211**, 100-108.
- Bruneau, B. G., Nemer, G., Schmitt, J. P., Charron, F., Robitaille, L., Caron, S., Conner, D. A., Gessler, M., Nemer, M., Seidman, C. E. et al. (2001). A murine model of Holt-Oram syndrome defines roles of the T-box transcription factor *Tbx5* in cardiogenesis and disease. *Cell* **106**, 709-721.
- Buckingham, M., Meilhac, S. and Zaffran, S. (2005). Building the mammalian heart from two sources of myocardial cells. *Nat. Rev. Genet.* **6**, 826-835.
- Chapman, G., Sparrow, D. B., Kremmer, E. and Dunwoodie, S. L. (2011). Notch inhibition by the ligand DELTA-LIKE 3 defines the mechanism of abnormal vertebral segmentation in spondylocostal dysostosis. *Hum. Mol. Genet.* **20**, 905-916.
- Chen, J., Kubalak, S. W., Minamisawa, S., Price, R. L., Becker, K. D., Hickey, R., Ross, J. and Chien, K. R. (1998). Selective requirement of myosin light chain 2v in embryonic heart function. *J. Biol. Chem.* **273**, 1252-1256.

- Chieffo, C., Garvey, N., Gong, W., Roe, B., Zhang, G., Silver, L., Emanuel, B. S. and Budarf, M. L. (1997). Isolation and characterization of a gene from the DiGeorge chromosomal region homologous to the MouseTbx1Gene. *Genomics* **43**, 267-277.
- Chun, H., Yue, Y., Wang, Y., Dawa, Z., Zhen, P., La, Q., Zong, Y., Qu, Y. and Mu, D. (2018). High prevalence of congenital heart disease at high altitudes in Tibet. *Eur. J. Prev. Cardiol.* 2047487318812502.
- Corrigan, N., Brazil, D. P. and McAuliffe, F. M. (2010). High-frequency ultrasound assessment of the murine heart from embryo through to juvenile. *Reprod. Sci.* **17**, 147-157.
- de Boer, B. A., van den Berg, G., de Boer, P. A. J., Moorman, A. F. M. and Ruijter, J. M. (2012). Growth of the developing mouse heart: an interactive qualitative and quantitative 3D atlas. *Dev. Biol.* **368**, 203-213.
- del Monte-Nieto, G., Ramialison, M., Adam, A. A. S., Wu, B., Aharonov, A., D'Uva, G., Bourke, L. M., Pitulescu, M. E., Chen, H., de la Pompa, J. L. et al. (2018). Control of cardiac jelly dynamics by NOTCH1 and NRG1 defines the building plan for trabeculation. *Nature* **557**, 439-445.
- Dewan, P. and Gupta, P. (2012). Burden of Congenital Rubella Syndrome (CRS) in India: a systematic review. *Indian Pediatr.* **49**, 377-399.
- Flores, L. E., Hildebrandt, T. B., Kühl, A. A. and Drews, B. (2014). Early detection and staging of spontaneous embryolysis by ultrasound biomicroscopy in murine pregnancy. *Reprod. Biol. Endocrinol.* **12**, 38.
- Furtado, M. B., Wilmanns, J. C., Chandran, A., Tonta, M., Biben, C., Eichenlaub, M., Coleman, H. A., Berger, S., Bouveret, R., Singh, R. et al. (2016). A novel conditional mouse model for Nkx2-5 reveals transcriptional regulation of cardiac ion channels. *Differentiation* **91**, 29-41.
- Hoch, R. V. (2006). Context-specific requirements for Fgfr1 signaling through Frs2 and Frs3 during mouse development. *Development* **133**, 663-673.
- Hoffman, J. I. (1995). Incidence of congenital heart disease: II. Prenatal incidence. *Pediatr. Cardiol.* **16**, 155-165.
- Ingalls, T. H., Curley, F. J. and Prindle, R. A. (1952). Experimental production of congenital anomalies; timing and degree of anoxia as factors causing fetal deaths and congenital anomalies in the mouse. *N. Engl. J. Med.* **247**, 758-768.
- Jay, P. Y., Harris, B. S., Maguire, C. T., Buerger, A., Wakimoto, H., Tanaka, M., Kupersmidt, S., Roden, D. M., Schultheiss, T. M., O'Brien, T. X. et al. (2004). Nkx2-5 mutation causes anatomic hypoplasia of the cardiac conduction system. *J. Clin. Invest.* **113**, 1130-1137.
- Jiang, B. H., Semenza, G. L., Bauer, C. and Marti, H. H. (1996). Hypoxia-inducible factor 1 levels vary exponentially over a physiologically relevant range of O₂ tension. *Am. J. Physiol.* **271**, C1172-C1180.
- Kopf, P. G. and Walker, M. K. (2009). Overview of developmental heart defects by dioxins, PCBs, and pesticides. *J. Environ. Sci. Health C* **27**, 276-285.
- Krishnan, J., Ahuja, P., Bodenmann, S., Knapik, D., Perriard, E., Krek, W. and Perriard, J.-C. (2008). Essential role of developmentally activated hypoxia-inducible factor 1alpha for cardiac morphogenesis and function. *Circ. Res.* **103**, 1139-1146.
- Li, Q. Y., Newbury-Ecob, R. A., Terrett, J. A., Wilson, D. I., Curtis, A. R. J., Yi, C. H., Gebuhr, T., Bullen, P. J., Robson, S. C., Strachan, T. et al. (1997). Holt-Oram syndrome is caused by mutations in TBX5, a member of the Brachyury (T) gene family. *Nat. Genet.* **15**, 21-29.
- Liang, Q., Gong, W., Zheng, D., Zhong, R., Wen, Y. and Wang, X. (2017). The influence of maternal exposure history to virus and medicine during pregnancy on congenital heart defects of fetus. *Environ. Sci. Pollut. Res. Int.* **24**, 5628-5632.
- Lindsay, E. A., Vitelli, F., Su, H., Morishima, M., Huynh, T., Pramparo, T., Jurecic, V., Ogunrinu, G., Sutherland, H. F., Scambler, P. J. et al. (2001). Tbx1 haploinsufficiency in the DiGeorge syndrome region causes aortic arch defects in mice. *Nature* **410**, 97-101.
- Macatee, T. L., Hammond, B. P., Arenkiel, B. R., Francis, L., Frank, D. U. and Moon, A. M. (2003). Ablation of specific expression domains reveals discrete functions of ectoderm- and endoderm-derived FGF8 during cardiovascular and pharyngeal development. *Development* **130**, 6361-6374.
- Marguerie, A., Bajolle, F., Zaffran, S., Brown, N. A., Dickson, C., Buckingham, M. E. and Kelly, R. G. (2006). Congenital heart defects in Fgfr2-IIIb and Fgf10 mutant mice. *Cardiovasc. Res.* **71**, 50-60.
- McElhinney, D. B., Geiger, E., Blinder, J., Benson, D. W. and Goldmuntz, E. (2003). NKX2.5 mutations in patients with congenital heart disease. *J. Am. Coll. Cardiol.* **42**, 1650-1655.
- Menendez-Montes, I., Escobar, B., Palacios, B., Gómez, M. J., Izquierdo-García, J. L., Flores, L., Jiménez-Borreguero, L. J., Aragones, J., Ruiz-Cabello, J., Torres, M. et al. (2016). Myocardial VHL-HIF signaling controls an embryonic metabolic switch essential for cardiac maturation. *Dev. Cell* **39**, 724-739.
- Mommersteeg, M. T. M., Hoogaars, W. M. H., Prall, O. W. J., de Gier-de Vries, C., Wiese, C., Clout, D. E. W., Papaioannou, V. E., Brown, N. A., Harvey, R. P., Moorman, A. F. M. et al. (2007). Molecular pathway for the localized formation of the sinoatrial node. *Circ. Res.* **100**, 354-362.
- Moreau, J. L. M., Artap, S. T., Shi, H., Chapman, G., Leone, G., Sparrow, D. B. and Dunwoodie, S. L. (2014). Cited2 is required in trophoblasts for correct placental capillary patterning. *Dev. Biol.* **392**, 62-79.
- Moumne, O., Chowdhury, R., Doll, C., Pereira, N., Hashimi, M., Grindrod, T., Dollar, J. J., Riva, A. and Kasahara, H. (2018). Mechanism sharing between genetic and gestational hypoxia-induced cardiac anomalies. *Front. Cardiovasc. Med.* **5**, 425.
- Mu, J. and Adamson, S. L. (2006). Developmental changes in hemodynamics of uterine artery, utero- and umbilicoplacental, and vitelline circulations in mouse throughout gestation. *Am. J. Physiol. Heart Circ. Physiol.* **291**, H1421-H1428.
- Nagao, K., Taniyama, Y., Kietzmann, T., Doi, T., Komuro, I. and Morishita, R. (2008). HIF-1alpha signaling upstream of NKX2.5 is required for cardiac development in *Xenopus*. *J. Biol. Chem.* **283**, 11841-11849.
- Naiche, L. A., Holder, N. and Lewandoski, M. (2011). FGF4 and FGF8 comprise the wavefront activity that controls somitogenesis. *Proc. Natl. Acad. Sci. USA* **108**, 4018-4023.
- Newbury-Ecob, R. A., Leanage, R., Raeburn, J. A. and Young, I. D. (1996). Holt-Oram syndrome: a clinical genetic study. *J. Med. Genet.* **33**, 300-307.
- O'Reilly, V. C., Lopes Floro, K., Shi, H., Chapman, B. E., Preis, J. I., James, A. C., Chapman, G., Harvey, R. P., Johnson, R. S., Grieve, S. M. et al. (2014). Gene-environment interaction demonstrates the vulnerability of the embryonic heart. *Dev. Biol.* **391**, 99-110.
- Park, E. J., Ogden, L. A., Talbot, A., Evans, S., Cai, C.-L., Black, B. L., Frank, D. U. and Moon, A. M. (2006). Required, tissue-specific roles for Fgf8 in outflow tract formation and remodeling. *Development* **133**, 2419-2433.
- Park, E. J., Watanabe, Y., Smyth, G., Miyagawa-Tomita, S., Meyers, E., Klingensmith, J., Camenisch, T., Buckingham, M. and Moon, A. M. (2008). An FGF autocrine loop initiated in second heart field mesoderm regulates morphogenesis at the arterial pole of the heart. *Development* **135**, 3599-3610.
- Perera, J. L., Johnson, N. M., Judge, D. P. and Crosson, J. E. (2014). Novel and highly lethal NKX2.5 missense mutation in a family with sudden death and ventricular arrhythmia. *Pediatr. Cardiol.* **35**, 1206-1212.
- Prall, O. W. J., Menon, M. K., Solloway, M. J., Watanabe, Y., Zaffran, S., Bajolle, F., Biben, C., McBride, J. J., Robertson, B. R., Chaulet, H. et al. (2007). An Nkx2-5/Bmp2/Smad1 negative feedback loop controls heart progenitor specification and proliferation. *Cell* **128**, 947-959.
- Prendiville, T., Jay, P. Y. and Pu, W. T. (2014). Insights into the genetic structure of congenital heart disease from human and murine studies on monogenic disorders. *Cold Spring Harb. Perspect. Med.* **4**, a013946.
- Raleigh, J. A., Chou, S.-C., Arteel, G. E. and Horsman, M. R. (1999). Comparisons among pimonidazole binding, oxygen electrode measurements, and radiation response in C3H mouse tumors. *Radiat. Res.* **151**, 580-589.
- Ramakrishnan, A., Lee, L. J., Mitchell, L. E. and Agopian, A. J. (2015). Maternal hypertension during pregnancy and the risk of congenital heart defects in offspring: a systematic review and meta-analysis. *Pediatr. Cardiol.* **36**, 1442-1451.
- Rana, M. S., Théveniau-Ruissy, M., De Bono, C., Mesbah, K., Francou, A., Rammah, M., Domínguez, J. N., Roux, M., Laforest, B., Anderson, R. H. et al. (2014). Tbx1 coordinates addition of posterior second heart field progenitor cells to the arterial and venous poles of the heart. *Circ. Res.* **115**, 790-799.
- Reamon-Buettner, S. M. and Borlak, J. (2010). NKX2-5: an update on this hypermutable homeodomain protein and its role in human congenital heart disease (CHD). *Hum. Mutat.* **31**, 1185-1194.
- Risebro, C. A., Petchey, L. K., Smart, N., Gomes, J., Clark, J., Vieira, J. M., Yanni, J., Dobrzynski, H., Davidson, S., Zuberi, Z. et al. (2012). Epistatic rescue of Nkx2.5 adult cardiac conduction disease phenotypes by prospero-related homeobox protein 1 and HDAC3. *Circ. Res.* **111**, e19-e31.
- Ruiz-Villalba, A., Mattiotti, A., Gunst, Q. D., Cano-Ballesteros, S., van den Hoff, M. J. B. and Ruijter, J. M. (2017). Reference genes for gene expression studies in the mouse heart. *Sci. Rep.* **7**, 24.
- Saint Hilaire, G. (1820). Différents états de pesanteur des oeufs au commencement et à la fin de l'incubation. *J. Comp. Sci. Med.* **7**, 271.
- Schulkey, C. E., Regmi, S. D., Magnan, R. A., Danzo, M. T., Luther, H., Hutchinson, A. K., Panzer, A. A., Grady, M. M., Wilson, D. B. and Jay, P. Y. (2015). The maternal-age-associated risk of congenital heart disease is modifiable. *Nature* **520**, 230-233.
- Shi, H., O'Reilly, V. C., Moreau, J. L. M., Bewes, T. R., Yam, M. X., Chapman, B. E., Grieve, S. M., Stocker, R., Graham, R. M., Chapman, G. et al. (2016). Gestational stress induces the unfolded protein response, resulting in heart defects. *Development* **143**, 2561-2572.
- Shi, H., Enriquez, A., Rapadas, M., Martin, E. M. M. A., Wang, R., Moreau, J., Lim, C. K., Szot, J. O., Ip, E., Hughes, J. N. et al. (2017). NAD deficiency, congenital malformations, and Niacin supplementation. *N. Engl. J. Med.* **377**, 544-552.
- Sparrow, D. B., Chapman, G. and Dunwoodie, S. L. (2011). The mouse notches up another success: understanding the causes of human vertebral malformation. *Mamm. Genome* **22**, 362-376.
- Sparrow, D. B., Chapman, G., Smith, A. J., Mattar, M. Z., Major, J. A., O'Reilly, V. C., Saga, Y., Zackai, E. H., Dormans, J. P., Alman, B. A. et al. (2012). A mechanism for gene-environment interaction in the etiology of congenital scoliosis. *Cell* **149**, 295-306.
- Sullivan, P. M., Dervan, L. A., Reiger, S., Buddhe, S. and Schwartz, S. M. (2015). Risk of congenital heart defects in the offspring of smoking mothers: a population-based study. *J. Pediatr.* **166**, 978-984.e2.

- Terada, R., Warren, S., Lu, J. T., Chien, K. R., Wessels, A. and Kasahara, H.** (2011). Ablation of *Nkx2-5* at mid-embryonic stage results in premature lethality and cardiac malformation. *Cardiovasc. Res.* **91**, 289-299.
- van der Linde, D., Konings, E. E. M., Slager, M. A., Witsenburg, M., Helbing, W. A., Takkenberg, J. J. M. and Roos-Hesselink, J. W.** (2011). Birth prevalence of congenital heart disease worldwide. *J. Am. Coll. Cardiol.* **58**, 2241-2247.
- van Weerd, J. H. and Christoffels, V. M.** (2016). The formation and function of the cardiac conduction system. *Development* **143**, 197-210.
- Vitelli, F., Taddei, I., Morishima, M., Meyers, E. N., Lindsay, E. A. and Baldini, A.** (2002). A genetic link between *Tbx1* and fibroblast growth factor signaling. *Development* **129**, 4605-4611.
- Vitelli, F., Lania, G., Huynh, T. and Baldini, A.** (2010). Partial rescue of the *Tbx1* mutant heart phenotype by *Fgf8*: genetic evidence of impaired tissue response to *Fgf8*. *J. Mol. Cell. Cardiol.* **49**, 836-840.
- Wang, G. L. and Semenza, G. L.** (1993). General involvement of hypoxia-inducible factor 1 in transcriptional response to hypoxia. *Proc. Natl. Acad. Sci. USA* **90**, 4304-4308.
- Watanabe, Y., Miyagawa-Tomita, S., Vincent, S. D., Kelly, R. G., Moon, A. M. and Buckingham, M. E.** (2010). Role of mesodermal *FGF8* and *FGF10* overlaps in the development of the arterial pole of the heart and pharyngeal arch arteries. *Circ. Res.* **106**, 495-503.
- Webster, W. S., Nilsson, M. and Ritchie, H.** (2014). Therapeutic drugs that slow the heart rate of early rat embryos. Is there a risk for the human? *Curr. Pharm. Des.* **20**, 5364-5376.
- Weissgerber, P., Held, B., Bloch, W., Kaestner, L., Chien, K. R., Fleischmann, B. K., Lipp, P., Flockerzi, V. and Freichel, M.** (2006). Reduced cardiac L-type Ca^{2+} current in *Cav2-/-* embryos impairs cardiac development and contraction with secondary defects in vascular maturation. *Circ. Res.* **99**, 749-757.
- Wren, C., Birrell, G. and Hawthorne, G.** (2003). Cardiovascular malformations in infants of diabetic mothers. *Heart* **89**, 1217-1220.
- Yagi, H., Furutani, Y., Hamada, H., Sasaki, T., Asakawa, S., Minoshima, S., Ichida, F., Joo, K., Kimura, M., Imamura, S.-I. et al.** (2005). Role of *TBX1* in human del22q11.2 syndrome. *Lancet* **362**, 1366-1373.
- Yu, K., Xu, J., Liu, Z., Sosic, D., Shao, J., Olson, E. N., Towler, D. A. and Ornitz, D. M.** (2003). Conditional inactivation of *FGF receptor 2* reveals an essential role for *FGF* signaling in the regulation of osteoblast function and bone growth. *Development* **130**, 3063-3074.
- Yu, C., Teoh, T. G. and Robinson, S.** (2006). Review article: obesity in pregnancy. *BJOG* **113**, 1117-1125.
- Yuan, X., Qi, H., Li, X., Wu, F., Fang, J., Bober, E., Dobрева, G., Zhou, Y. and Braun, T.** (2017). Disruption of spatiotemporal hypoxic signaling causes congenital heart disease in mice. *J. Clin. Invest.* **127**, 2235-2248.
- Zheng, J.-Y., Tian, H.-T., Zhu, Z.-M., Li, B., Han, L., Jiang, S.-L., Chen, Y., Li, D.-T., He, J.-C., Zhao, Z. et al.** (2013). Prevalence of symptomatic congenital heart disease in Tibetan school children. *Am. J. Cardiol.* **112**, 1468-1470.
- Zhou, B., Si, W., Su, Z., Deng, W., Tu, X. and Wang, Q.** (2013). Transcriptional activation of the *Prox1* gene by *HIF-1 α* and *HIF-2 α* in response to hypoxia. *FEBS Lett.* **587**, 724-731.
- Zhu, H., Kartiko, S. and Finnell, R. H.** (2009). Importance of gene-environment interactions in the etiology of selected birth defects. *Clin. Genet.* **75**, 409-423.

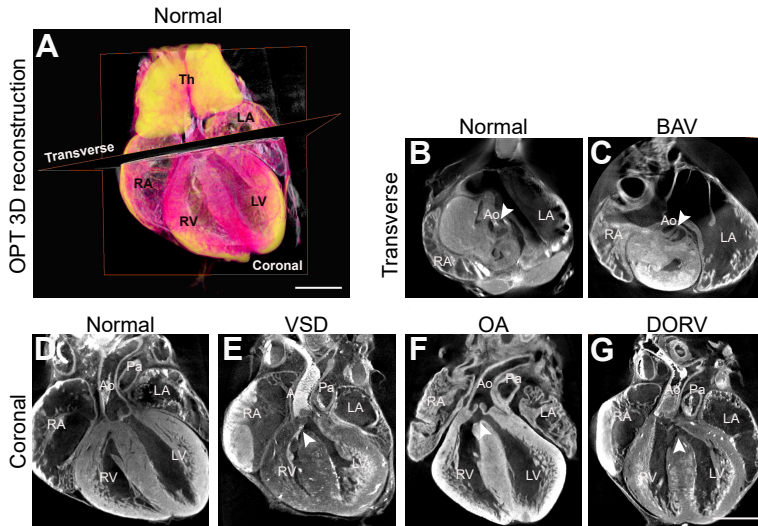


Figure S1: Representative images of heart defect assessment of E17.5 embryos using OPT imaging and 3D reconstruction.

(A) 3D reconstruction of a normal E17.5 mouse embryonic heart. (B-C) Representative images of cardiac transverse sections of a normal tricuspid aortic valve (B, arrowhead) and a bicuspid aortic valve (C, BAV, arrowhead). (D-G) Representative images of cardiac coronal sections of a normal heart (D) and heart displaying a ventricular septal defect (E, VSD, arrowhead), an overriding aorta (F, OA, arrowhead) and a double outlet right ventricle (G, DORV, arrowhead). RA: right atrium, LA: left atrium, RV: right ventricle, LV: left ventricle, Ao: Aorta, Pa: pulmonary artery, Th: thymi. The scale bar represents 0.5 mm

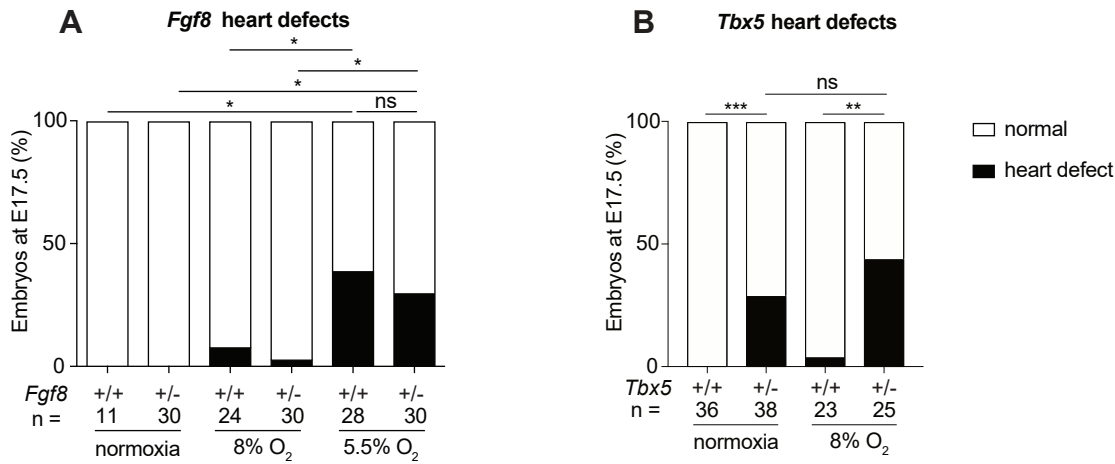


Figure S2: Incidence of heart defects in embryos with mutated cardiac development genes following maternal exposure to low oxygen. Histograms showing the percentage of heart defects present in E17.5 embryos following maternal exposure to the indicated level of hypoxia at E9.5. (A) *Fgf8* and (B) *Tbx5*. Data were tested for statistical significance by two-tailed Fisher's exact test. All relevant pairs were statistically tested and only the significant and/or relevant ones are shown. ns not significant, * $P < 0.05$, ** $P < 0.01$, *** $P < 0.001$.

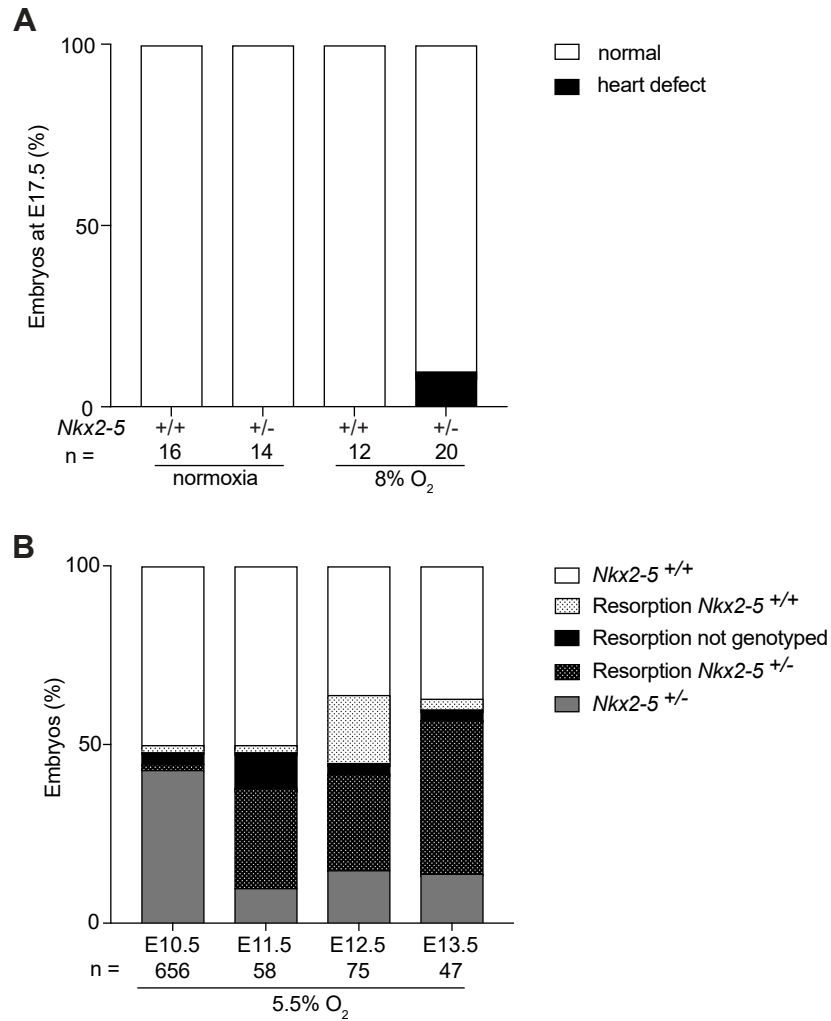


Figure S3: Embryonic survival and resorption genotypes following maternal exposure to low oxygen. (A) Histograms showing the percentage of heart defects present in E17.5 *Nkx2-5* embryos following maternal exposure to 8% Oxygen at E9.5. (B) Histogram showing the percentage of *Nkx2-5*^{+/+} embryos alive (white), *Nkx2-5*^{+/+} resorbed (white with dots), *Nkx2-5*^{+/-} alive (grey), *Nkx2-5*^{+/-} resorbed (black with dots) and the resorptions that could not be genotyped (black) exposed to 5.5% Oxygen at the indicated developmental stages.

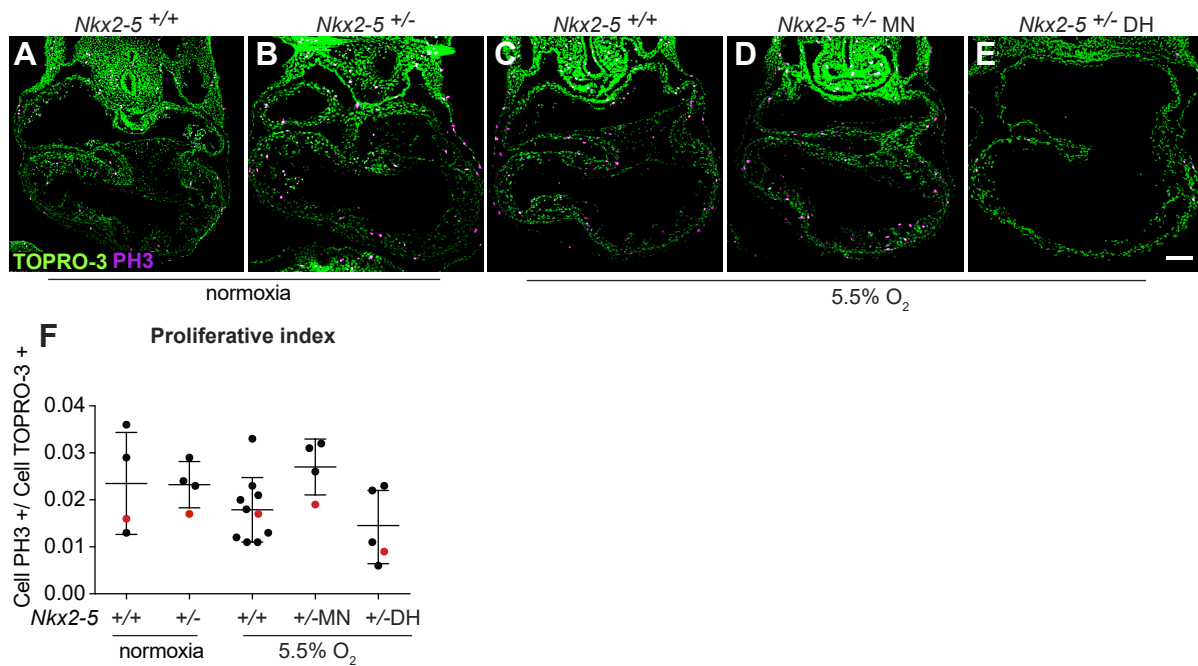


Figure S4: Proliferative index of *Nkx2-5* embryos following maternal exposure to low oxygen. (A-E) Comparison of Phospho-HISTONE H3 expression (magenta) in *Nkx2-5*^{+/+} controls (A, n=4), *Nkx2-5*^{+/-} controls (B, n=4), and exposed to 5.5% oxygen *Nkx2-5*^{+/+} (C, n=10), *Nkx2-5*^{+/-} with a morphologically normal heart (D, n=4) and *Nkx2-5*^{+/-} with a dilated heart (E, n=5). Nuclei are stained with TOPRO-3 (green). (F) Quantification of phospho-histone H3-positive nuclei. Red dots indicate quantification of the images shown in A-E. Data were tested for statistical significance by one-way ANOVA with Tukey's *post hoc* test. Error bars show standard deviations. DH: dilated heart, MN: morphologically normal heart. The scale bar represents 100 μ m.

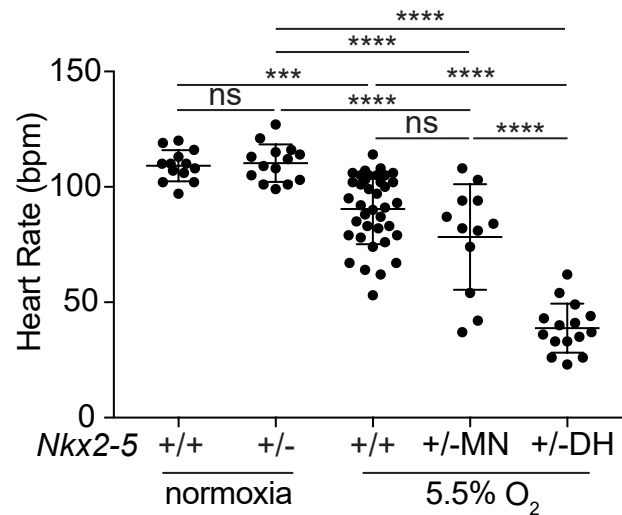
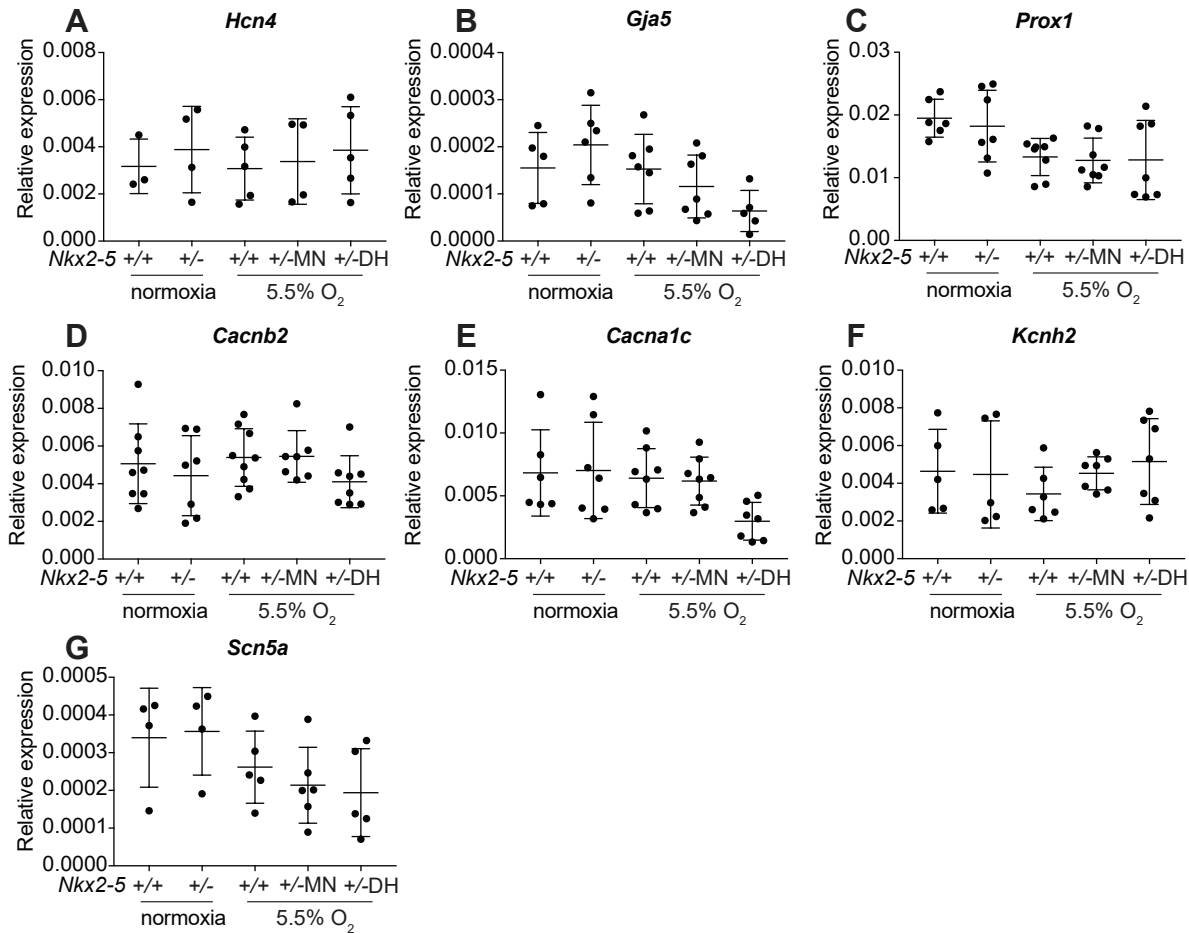
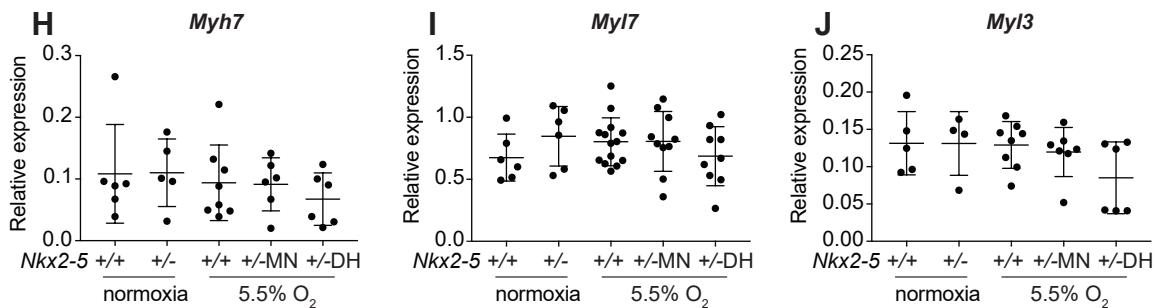


Figure S5: *In utero* embryonic cardiac chronotropy assessment. Quantification of the heart rate of each embryo in the given genotypes and conditions at E10.5. Data were tested for statistical significance by one-way ANOVA with Tukey's *post hoc* test. Error bars show standard deviations. ns not significant, *** $P < 0.001$, **** $P < 0.0001$. DH: dilated heart, MN: morphologically normal heart, bpm: beats per minute.

CONDUCTION SYSTEM



CONTRACTILITY



OTHER

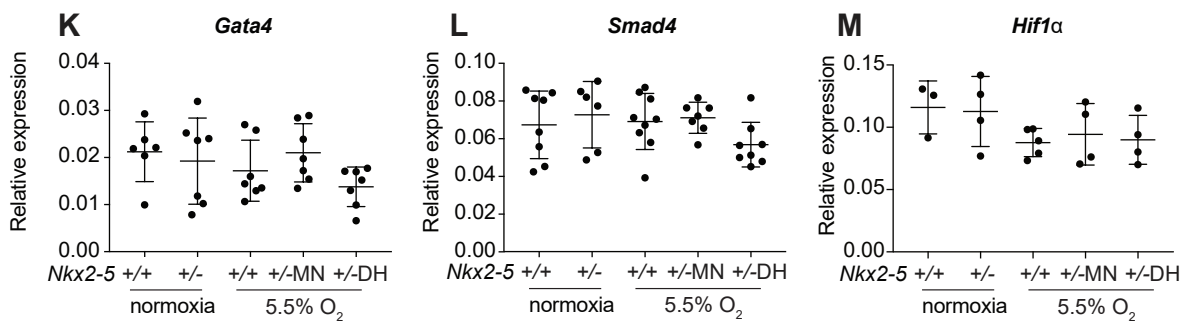
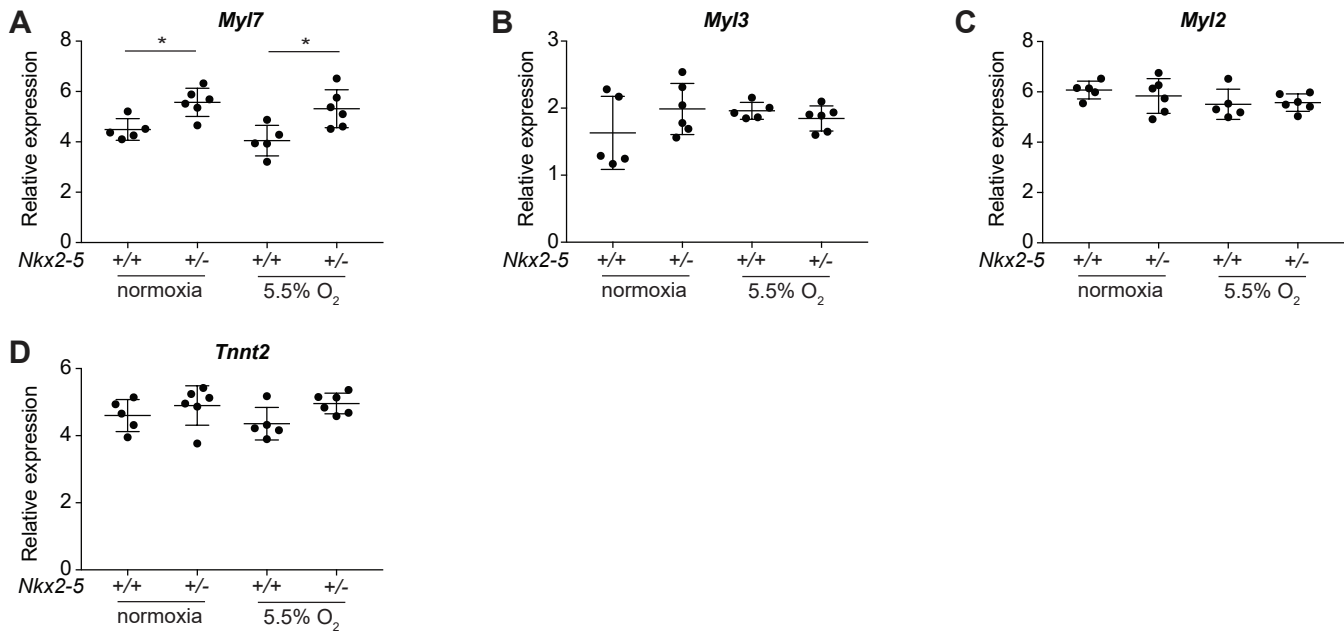


Figure S6: Effects of maternal exposure to low oxygen on embryonic levels of cardiac gene transcripts at E10.5. (A-J) Quantification of transcript levels of (A) *Hcn4*, (B) *Gja5*, (C) *Prox1*, (D) *Cacnb2*, (E) *Cacna1c*, (F) *Kcnh2*, (G) *Scn5a*, (H) *Myh7*, (I) *Myl7*, (J) *Myl3*, (K) *Gata4*, (L) *Smad4* and (M) *Hif1a* at E10.5 by qPCR relative to *Gapdh* and *Eef1e1*. Data were tested for statistical significance by one-way ANOVA with Tukey's *post hoc* test. Error bars show standard deviations. DH: dilated heart, MN: morphologically normal heart.

CONTRACTILITY



CONDUCTION SYSTEM

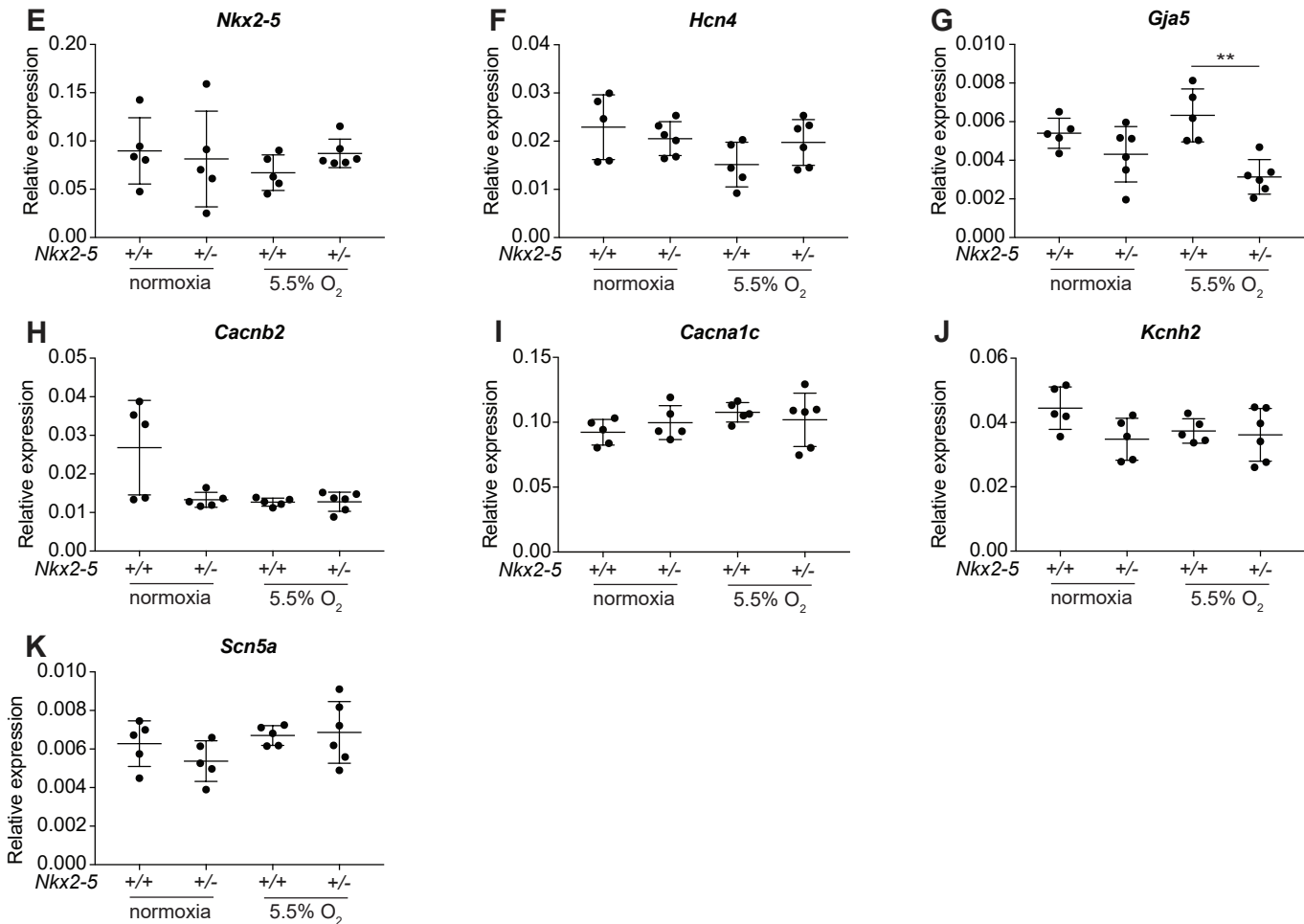


Figure S7: Effects of maternal exposure to low oxygen on embryonic levels of cardiac gene transcripts at E12.5. (A-K) Quantification of transcript levels of (A) *Myl7*, (B) *Myl3*, (C) *Myl2*, (D) *Tnnt2*, (E) *Nkx2-5*, (F) *Hcn4*, (G) *Gja5*, (H) *Cacnb2*, (I) *Cacna1c*, (J) *Kcnh2*, and (K) *Scn5a* at E12.5 by qPCR relative to *Gapdh* and *Eef1e1*. Data were tested for statistical significance by one-way ANOVA with Tukey's *post hoc* test. Error bars show standard deviations. DH: dilated heart, MN: morphologically normal heart. * $P < 0.05$, ** $P < 0.01$.

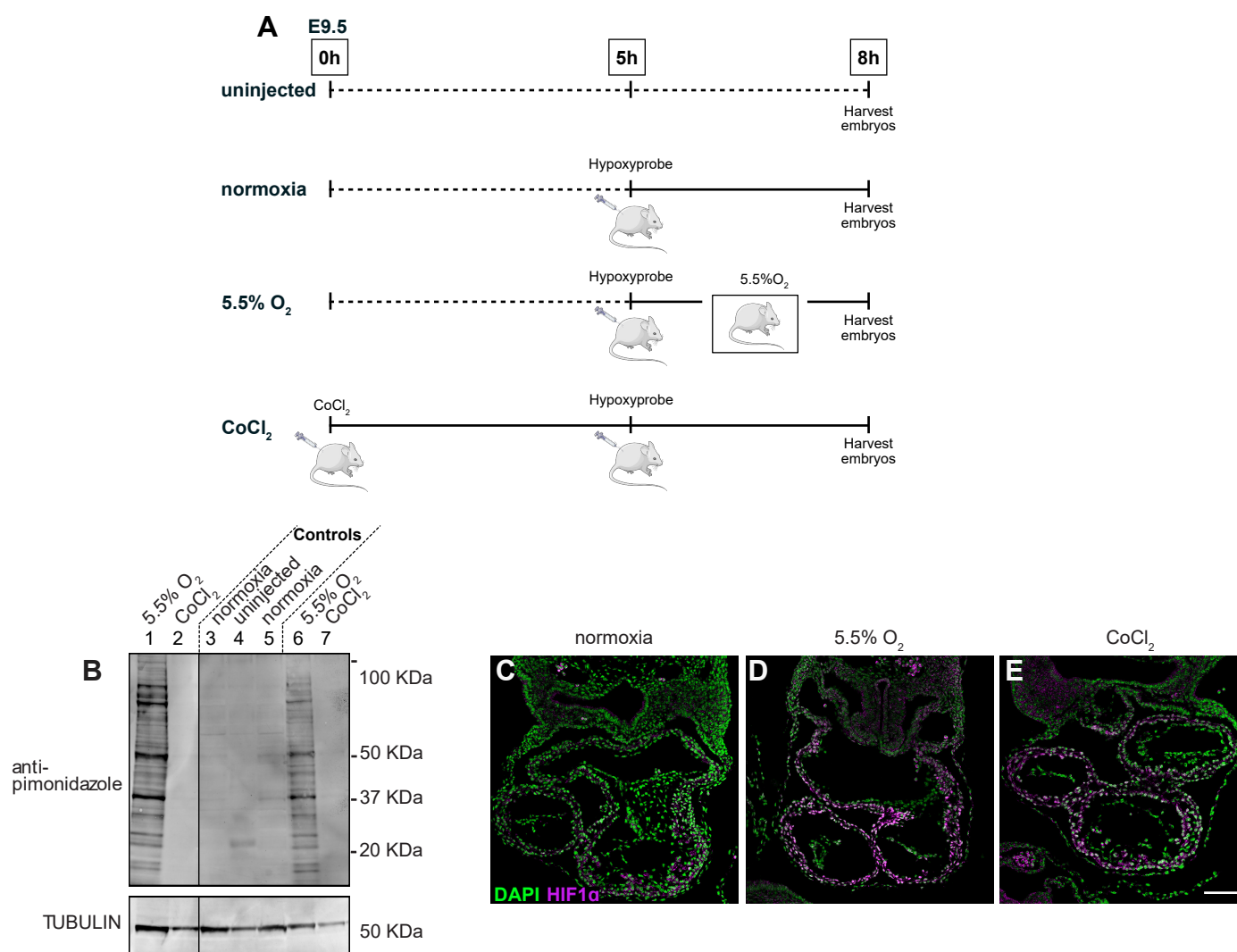


Figure S8: Induction of hypoxia and accumulation of HIF1 α in embryonic heart following maternal cobalt chloride injection in wildtype E9.5 embryos. (A) Schematic diagram illustrating the experimental design. (B) Western Blot showing quantification of HypoxypromeTM adducts in E9.5 embryo. Embryos were uninjected (n=1, lane 4), normoxic (n=2, lane 3 and 5), exposed to 5.5% O₂ for 3 hours (n=2, lanes 1 and 6), and 8 hours after injection of 40mg/kg cobalt chloride (n=2, lanes 2 and 7). β -TUBULIN was used as the loading control. (C-E) Comparison of expression levels of HIF1 α (magenta) in control embryos (C, n=2), embryos after 3 hours maternal exposure to low oxygen (D, n=2), and embryos 8 hours after maternal cobalt chloride injection (E, n=2). The scale bar represents 100 μ m in C-E.

					Type of heart defect observed												
O ₂ %	Embryo genotype		Embryos examined	Normal	Abnormal	VSD	Musc VSD	OA	DORV	BAV	ASD	TGA	SOTV	PTA	EC	HRH	
21%	Fgf8		+/+	11	11	0	0	0	0	0	0	0	0	0	0	0	
			+/-	30	30	0	0	0	0	0	0	0	0	0	0	0	0
8%			+/+	24	22	2	0	2	0	0	0	0	0	0	0	0	0
			+/-	30	29	1	0	1	0	0	0	0	0	0	0	0	0
5.5%			+/+	28	17	11	10	0	6	1	1	0	0	0	0	1	0
			+/-	30	21	9	8	0	2	1	1	0	2	1	0	0	0
21%	FgfR1		FgfR2		+/+	20	20	0	0	0	0	0	0	0	0	0	
					+/-	21	21	0	0	0	0	0	0	0	0	0	
					+/+	20	20	0	0	0	0	0	0	0	0	0	
					+/-	22	22	0	0	0	0	0	0	0	0	0	
8%			+/+	52	48	4	2	1	1	1	1	0	0	0	0	0	0
			+/-	37	33	4	3	1	1	0	1	0	0	0	0	0	0
			+/+	42	39	3	3	1	1	1	1	0	0	0	0	0	0
			+/-	34	25	9	7	1	1	0	1	0	0	0	0	0	1

Table S1: Pregnant mice were exposed at the indicated oxygen concentration for 8 hours at E9.5 days of gestation. Mice were returned to normoxia, and embryos allowed to develop until E17.5, when heart morphology was analysed using OPT in 3D. VSD: membranous ventricular septal defect; muscVSD: muscular ventricular septal defect; OA: overriding aorta; DORV: double-outlet right ventricle; TGA: transposition of the great arteries; ASD: atrial septal defect; PTA: persistent truncus arteriosus; SOTV: straddling overriding tricuspid valve; BAV: bicuspid aortic valve; EC: ectopia cordis; HRH: hypoplastic right heart. Note that a particular embryo may have more than one type of defect. The heart defects in bold are more severe than the ones in regular font. Also see Figure S1 for representative images of heart defects.

O ₂ %	Embryo genotype	Embryos examined	Normal	Abnormal	Type of heart defect observed										
					VSD	Musc VSD	OA	DORV	BAV	ASD	TGA	SOTV	PTA	HLH	
21%	Tbx5	+/+	36	36	0	0	0	0	0	0	0	0	0	0	0
		+/-	38	27	11	5	0	3	1	0	3	0	3	1	2
8%	Tbx5	+/+	23	22	1	1	0	1	0	0	0	0	0	0	0
		+/-	25	14	11	4	3	5	2	0	1	0	1	1	2
21%	Tbx1	+/+	11	11	0	0	0	0	0	0	0	0	0	0	0
		+/-	20	19	1	1	0	0	0	0	0	0	0	0	0
8%	Tbx1	+/+	32	31	1	1	0	0	0	0	0	0	0	0	0
		+/-	37	35	2	0	2	0	0	0	0	0	0	0	0
5.5%	Tbx1	+/+	43	27	16	4	3	5	1	0	0	1	0	1	0
		+/-	31	8	23	8	3	8	3	0	0	1	0	0	0
21%	Nkx2-5	+/+	16	16	0	0	0	0	0	0	0	0	0	0	0
		+/-	14	14	0	0	0	0	0	0	0	0	0	0	0
8%	Nkx2-5	+/+	12	12	0	0	0	0	0	0	0	0	0	0	0
		+/-	20	18	2	1	0	0	0	0	1	0	0	0	0

Table S2: Pregnant mice were exposed at the indicated oxygen concentration for 8 hours at E9.5 days of gestation. Mice were returned to normoxia, and embryos allowed to develop until E17.5, when heart morphology was assessed using OPT in 3D. VSD: membranous ventricular septal defect; muscVSD: muscular ventricular septal defect; OA: overriding aorta; DORV: double-outlet right ventricle; BAV: bicuspid aortic valve; ASD: atrial septal defect; TGA: transposition of the great arteries; SOTV: straddling overriding tricuspid valve; PTA: persistent truncus arteriosus; HLH: hypoplastic left heart. The heart defects in bold are more severe than the ones in regular font.

	Embryonic stage after exposure at E9.5 to 5.5% oxygen for 8 hours													
	E9.5 0h after 5.5%O ₂		E9.5 – E10 5h after 5.5%O ₂			E10.5			E11.5		E12.5		E17.5	
<i>Nkx2-5</i>	+/+	+/-	+/+	+/-		+/+	+/-		+/+	+/-	+/+	+/-	+/+	+/-
HIF1 α	=	=	↓	↑↑										
Live embryos (%)	100	100	100	100		96	96		96	27	66	25	94	18
	(F6)		(F6)			(F2, FS3)			(F2, FS3)		(F2, FS3)		(F1)	
Heart morphology (%)	normal 100	normal 100	normal 100	normal 55	DH 45	normal 100	normal 50	DH 50	normal 100	normal 100	normal 100	normal 100	normal 100	normal 100
	(F6)		(F6)			(F2)			(F2)		(F2)		(FS3)	
Nkx2-5 expression						=	↓	↓↓						
						(F3)								
Proliferation/apoptosis						=	=	=						
						(FS4)								
Heart rate						↓	↓↓	↓↓↓						
						(F4, FS5)								
Conduction						=	=	=			=	=		
						(FS6)					(FS7)			
Contractility						=	↓	↓↓			=	=		
						(F5, FS6)					(FS7)			

Table S3: Summary of molecular and morphological cardiac phenotype of *Nkx2-5* embryos following maternal low oxygen exposure. Embryonic day (E), figure (F), supplementary figure (FS), equal levels (=), elevated levels (↑), reduced levels (↓), wildtype (+/+), heterozygous null (+/-), dilated heart (DH).

Candidate	RefSeq	Primer Sequence	Reference
<i>Nkx2-5</i>	NM_008700.2	AAGTGCTCTCCTGCTTTCCC GCGCGCACAGCTCTTTTT	This study
<i>Myh7 (Beta-MHC)</i>	NM_001361607.1 NM_080728.3	CCTTACTTGCTACCCTCAGGTG GGCTGAGCCTTGGATTCTCAA	This study
<i>MyI7 (MLC2a)</i>	NM_022879.2	GGCACAACGTGGCTCTTCTAA TGCAGATGATCCCATCCCTGT	(Koren et al., 2013)
<i>MyI3 (MLC1v)</i>	NM_001364484.1 NM_010859.3	GGAAGCCGAGTTTGATGCC GCCTCCTTGAACTCTTCAATCT	This study
<i>Actc1</i>	NM_009608.4	GAACCACAGGCATTGTTCTGG CGCATGATGGCATGGGGTAA	This study
<i>MyI2 (MLC2v)</i>	NM_010861.4	ATCGACAAGAATGACCTAAGGGA ATTTTTACGTTCACTCGTCCT	(Koren et al., 2013)
<i>Tnnt2 (cTNT)</i>	NM_001130174.2 NM_001130175.2 NM_001130176.1 NM_001130177.2 NM_001130178.2 NM_001130179.2 NM_001130180.2 NM_001130181.2 NM_011619.3	ATGATGCACTTTGGAGGGTACA GGCCTTCTCTCTCAGTTGGT	This study
<i>Hcn4</i>	NM_001081192.1	CAGCGTCAGAGCGGATACTT CTTCTTGCCATGCGGTCCA	This study
<i>Gja5 (Cx40)</i>	NM_001271628.1 NM_008121.3	AGCTCTAAACGTGGAAGGCTC CCGATGACTGTGGAGTGCTT	This study
<i>Prox1</i>	NM_001360827.1 NM_008937.3	AAAGTCAAATGTACTCCGCAAGC CTGGGAAATTATGGTTGCTCCT	(Zhou et al., 2013)
<i>Cacnb2</i>	NM_001309519.1 NM_001252533.1 NM_023116.4	TCTCGAGGGAAATCTCAAGCA ATTCCTGCGGAGGACATTGG	This study
<i>Cacna1c</i>	NM_001159533.2 NM_001159534.2 NM_001159535.2 NM_001255997.2 NM_001255998.2 NM_001255999.2 NM_001256000.2 NM_001256001.2 NM_001256002.2 NM_001290335.1 NM_009781.4	CATGAAGCTCAACTCAACTGTTTC CGTGGGCTCCCATAGTTG	(Furtado et al., 2017)
<i>Kcnh2</i>	NM_001294162.1 NM_013569.2	GATCGCCTTCTACCGGAAA CATTCTTCACGGGTACCACA	(Furtado et al., 2017)
<i>Scn5a</i>	NM_001253860.1 NM_021544.4	GATGAGGAGAACAGCCTTGG CACAACTTGGGATTCTGCT	(Furtado et al., 2016)
<i>Gata4</i>	NM_001310610.1 NM_008092.4	GCTCCATGTCCAGACATTC ATGCATAGCCTTGTGGGGAC	This study
<i>Smad4</i>	NM_008540.2	CCAAGCGCGTATATAAAGGTCT GAGCTATTCCACCCACGGAC	This study
<i>Hif1α</i>	NM_001313919.1 NM_001313920.1 NM_010431.2	TCATCAGTTGCCACTTCCCC CTGTCTAGACCACCGGCATC	This study

Table S4: Primer sequences used for qPCR

Target	Name	Catalogue number	Species and type	Supplier	Dilution for IHC	Dilution for IB
Primary Antibodies						
α -Smooth Muscle-FITC	clone 1A4	F3777	Mouse monoclonal	Sigma-Aldrich	1:1,000	na
Phospho-histone H3	(Ser 10)- R	sc-8656	Rabbit polyclonal	Santa Cruz Biotechnology	1:200	na
NKX2-5		13921-1-AP	Rabbit polyclonal	Proteintech	na	1:1,000
β -Tubulin	Clone TUB 2.1	T5201	Mouse monoclonal	Sigma-Aldrich	na	1:5,000
HIF1 α		NB100-449	Rabbit polyclonal	Novus Biologicals	1:400	na
Hypoxyprobe TM	4.3.11.3		Mouse monoclonal	Hypoxyprobe, Inc.	1:500	na
Secondary Antibodies						
Donkey anti-rabbit Cy TM 3		711-165-152		Jackson ImmunoResearch	1:500	na
Donkey anti-mouse AlexaFluor [®] 488		715-545-151		Jackson ImmunoResearch	1:500	na
Goat anti-mouse IRDye [®] 800CW		926-32210		LI-COR	na	1:10,000
Donkey anti-rabbit biotinylated		711-065-152		Jackson ImmunoResearch	1:500	na
Tertiary reagents						
Streptavidin Cy TM 3		GTX8590 2		GeneTex	1:1,000	na
Nuclear stain						
TO-PRO [®] -3 Iodide		T3605		Life Technologies	1:10,000	na
DAPI		1023627 6001		Sigma-Aldrich	1:1,000	na

Table S5: Antibodies used for immunodetection